

ON THE SPECTRAL STABILITY OF SOLITARY WAVES

A Dissertation

by

RUOMENG LAN

Submitted to the Office of Graduate and Professional Studies of
Texas A&M University

in partial fulfillment of the requirements for the degree of

DOCTOR OF PHILOSOPHY

Chair of Committee,	Andrew Comech
Co-Chair of Committee,	Alexei Poltoraski
Committee Members,	Artem Abanov
	Gregory Berkolaiko
Head of Department,	Sarah Witherspoon

December 2019

Major Subject: Mathematics

Copyright 2019 Ruomeng Lan

ABSTRACT

We study the spectral stability of the solitary wave solutions to the nonlinear Dirac equations. We focus on two types of nonlinearity: the Soler type and the Coulomb type. For the Soler model, we apply the Evans function technique to explore the point spectrum of the linearized operator at a solitary wave solution to the 2D and 3D cases. For the toy Coulomb model, the solitary wave solutions are no longer $\mathbf{SU}(1, 1)$ symmetric. We show numerically that there are no eigenvalues near $2\omega i$ in the nonrelativistic limit ($\omega \lesssim m$) and the spectral stability persists in spite of the absence of $\mathbf{SU}(1, 1)$ symmetry.

DEDICATION

To my wife Yao and my son Xiao.

ACKNOWLEDGMENTS

I would like to express my deepest gratitude to my advisor, Dr. Andrew Comech, for introducing me to the nonlinear Dirac equation and the spectral theory. I appreciate his patience and encouragement. I cannot complete the dissertation without his guidance and help.

I would like to thank the committee member, Dr. Alexei Poltoratski, Dr. Gregory Berkolaiko and Dr. Arterm Abanov for offering their time and support. I thank Dr. Ciprian Foias and Dr. Edriss Titi for their excellent lectures on Navier-Stokes equations. I thank Ms. Monique Stewart for her help and consideration.

I would like to thank my parents for their selfless love and support.

CONTRIBUTORS AND FUNDING SOURCES

Contributors

This work was supported by a dissertation committee consisting of Professor Andrew Comech [advisor], Professor Alexei Poltoraski [co-advisor] and Professor Gregory Berkolaiko of the Department of Mathematics and Professor Artem Abanov of the Department of Physics.

Chapters 2 and 3 are based on the joint work with J. Cuevas-Maraver, P.G. Kevrekidis, A. Saxena and A. Comech, which was published in [1].

All other work conducted for the dissertation was completed by the student independently.

Funding Sources

Graduate study was supported by a teaching assistantship from Texas A&M University.

NOMENCLATURE

NLD	Nonlinear Dirac equation
NLS	Nonlinear Schrödinger equation
L^p	Space of functions with Lebesgue-integrable p th power of the absolute value
nD	n spatial dimensions
MTM	massive Thirring model
\mathbb{R}^n	n -dimensional real vector space
\mathbb{R}^+	Set of positive real numbers
\mathbb{C}^n	n -dimensional complex vector space
\bar{a}	Complex conjugate of the complex number a
$\operatorname{Re}(a)$	Real part of a complex number a
$\operatorname{Im}(a)$	Imaginary part of a complex number a
A^T	Transpose of a matrix A
A^*	the Hamiltonian conjugate of the operator A ; if A is a matrix, $A^* = (\bar{A})^T$
\mathcal{C}^n	Space of functions with continuous n th derivatives
\mathbb{N}	Set of all the positive integers
ODE	Ordinary differential equation
PDE	Partial differential equation
$\mathcal{L}(\mathcal{H})$	Space of linear operators on the space \mathcal{H}
$H^k(\Omega)$	Sobolev space $\{f \in L^2(\Omega) : \ \langle \xi \rangle^k \hat{f}(\xi)\ _{L^2(\Omega)} < +\infty\}$ where $\langle \xi \rangle := \sqrt{1 + \xi ^2}$, $\hat{f}(\xi)$ is the Fourier transform of $f(x)$ and $\Omega = \mathbb{R}^n$

TABLE OF CONTENTS

	Page
ABSTRACT	ii
DEDICATION	iii
ACKNOWLEDGMENTS	iv
CONTRIBUTORS AND FUNDING SOURCES	v
NOMENCLATURE	vi
TABLE OF CONTENTS	vii
LIST OF FIGURES	ix
1. INTRODUCTION.....	1
1.1 Dirac Operator.....	1
1.2 Nonlinear Dirac Equation.....	4
1.3 Solitary Waves.....	5
1.4 Stability Analysis	8
2. 2D SOLER MODEL	12
2.1 The Model	12
2.2 Linearization	15
2.3 Evans Function and Jost Solution	18
2.3.1 Introduction	19
2.3.2 A Simple Example	19
2.3.3 1D Soler Model.....	21
2.4 Evans function Factorization	23
2.5 Spectral Stability Analysis	25
2.5.1 Some Explicit Eigenvalues.....	25
2.5.2 Symmetry Properties for $\sigma_p(\mathcal{A})$	27
2.5.3 Essential Spectrum of \mathcal{A}	29
2.5.4 Construction of the Evans Function	31
2.5.5 Numerical Results	37
2.6 Conclusion.....	44
3. 3D SOLER MODEL	45

3.1	The Model	45
3.2	Linearization	47
3.3	Spectral Stability Analysis	50
3.3.1	Explicit Eigenvalue and Essential Spectrum of \mathcal{A}	50
3.3.2	Construction of the Evans Function	51
3.3.3	Numerical Results	53
3.4	Conclusion.....	55
3.4.1	Future work	55
4.	COULOMB-TYPE MODEL	57
4.1	The Model	57
4.2	The Existence of the Solitary Wave Solutions	58
4.3	Linearization	62
4.4	Spectral Stability Analysis	64
4.4.1	Essential Spectrum and Symmetry Properties	64
4.4.2	Eigenvalues near $2\omega_i$ in the Nonrelativistic Limit	64
4.5	Conclusion.....	71
5.	SUMMARY	72
	REFERENCES	73

LIST OF FIGURES

FIGURE	Page
2.1	Numerical solutions u and v for different values of ω in the 2D Soler model. Here we set $m = 1$ and $f(s) = s$ 14
2.2	The strip between the blue lines interpret the domain to search for the eigenvalues. The red lines stand for $\sigma_{\text{ess}}(\mathcal{A})$. The green stars stand for the threshold points. 39
2.3	Dependence of the imaginary (red asterisks) and real (green circles) parts of the eigenvalues corresponding to \mathcal{A}_0 of ω for solitary waves in the 2D Soler model. Here we set $m = 1$ and $f(s) = s$. The triangle above the blue line corresponds to the essential spectrum of \mathcal{A}_0 40
2.4	Dependence of the imaginary (red asterisks) and real (green circles) parts of the eigenvalues corresponding to $\mathcal{A}_{\pm 1}$ of ω for solitary waves in the 2D Soler model. Here we set $m = 1$ and $f(s) = s$. The triangle above the blue line corresponds to the essential spectrum of $A_{\pm 1}$. The eigenvalues embedded into the essential spectrum are ignored. 41
2.5	Dependence of the imaginary (red asterisks) and real (green circles) parts of the eigenvalues corresponding to $\mathcal{A}_{\pm 2}$ of ω for solitary waves in the 2D Soler model. Here we set $m = 1$ and $f(s) = s$. The triangle above the blue line corresponds to the essential spectrum of $A_{\pm 2}$ 42
2.6	Dependence of the imaginary (red asterisks) and real (green circles) parts of the eigenvalues corresponding to $\mathcal{A}_{\pm 3}$ with respect to ω of solitary waves in the 2D Soler model. Here we set $m = 1$ and $f(s) = s$. The triangle above the blue line represents the essential spectrum of $A_{\pm 3}$ 43
3.1	Numerical solutions u and v for different values of ω in the 3D Soler model. Here we set $m = 1$ and $f(s) = s$ 47
3.2	Dependence of the imaginary (red asterisks) and real (green circles) parts of the eigenvalues corresponding to \mathcal{A} with respect to ω of solitary waves in the 3D Soler model. Here we set $m = 1$ and $f(s) = s$. The triangle above the blue line represents the essential spectrum of A 54
4.1	Numerical solutions u and v to the system (4.4) for the frequency ω close to $m = 1$. 60
4.2	Differences of the profile functions between the Soler model and Coulomb model for the frequency ω close to $m = 1$ 66

- 4.3 The eigenvalues are searched in the region bounded by the blue dash lines for the frequency $\omega \in (0, 975m, 0.99m)$. The red interval represents the values $2\omega i$ corresponding to $\omega \in (0, 975m, 0.99m)$ 68
- 4.4 Dependence of the imaginary (red asterisks) and real (green circles) parts of resonances in the toy Coulomb model. The pink dash line and blue dash line stand for the threshold $(m + \omega)i$ and the value $2\omega i$, respectively. 70

1. INTRODUCTION

In this chapter, we introduce the nonlinear Dirac equations, solitary waves, and the spectral stability briefly. A short review for the related results is given as well.

1.1 Dirac Operator

The famous Dirac equation [2] describes the relativistic motion of a spin- $\frac{1}{2}$ particle in \mathbb{R}^3 , correctly taking into account their interaction with the external electromagnetic fields, as opposed to the Klein-Gordon equation which describes particles of zero spin. The Klein-Gordon equation (which for simplicity we write without the external electromagnetic fields),

$$-\frac{\partial^2}{\partial t^2}\psi(x, t) = (-\Delta + m^2)\psi(x, t), \quad t \geq 0, \quad x \in \mathbb{R}^3, \quad (1.1)$$

where m is the mass, is obtained from the classical relativistic energy-momentum relation for the energy E and the momentum p :

$$E^2 = p^2 + m^2. \quad (1.2)$$

We employ the units such that the speed of light c and the Plank's constant \hbar are both equal to one throughout the thesis. According to Schrödinger, the transition from the classical to the quantum mechanics is achieved by the substitution

$$E \longrightarrow i\frac{\partial}{\partial t}, \quad p \longrightarrow -i\nabla. \quad (1.3)$$

Dirac looked for a relativistically invariant equation which would allow one to exclude negative energies from the consideration, keeping the "positive" root of the $E^2 = p^2 + m^2$ energy-momentum relation. He ended up with the first order equation which still contained negative energies, but at the same time presented the consistent description to the internal structure of the electron (which was proposed back in 1924 by Wolfgang Pauli and in 1925 by George Uhlenbeck and Samuel

Goudsmit) [3] . In 1927, Dirac [2] tried to express E as

$$E = \sum_{i=1}^3 \alpha_i p_i + \beta m \quad (1.4)$$

so that the new E would still satisfy the relation (1.2). Thus, the matrices $\alpha_i, i = 1, 2, 3$ and β should satisfy the following relations

$$\alpha_i \alpha_k + \alpha_k \alpha_i = 2\delta_{ik} \mathbf{1}, \quad i, k = 1, 2, 3, \quad (1.5)$$

$$\alpha_i \beta + \beta \alpha_i = \mathbf{0}, \quad i = 1, 2, 3, \quad (1.6)$$

$$\beta^2 = \mathbf{1}, \quad (1.7)$$

where δ_{ik} denotes the Kronecker delta, $\mathbf{1}$ and $\mathbf{0}$ are the n -dimensional identity and zero matrices. By Equations (1.5) and (1.6) $\alpha_i, i = 1, 2, 3$ and β anti-commute with each other. Dirac noticed that

$$\left(\sum_{i=1}^3 \sigma_i p_i \right)^2 = \sum_{i=1}^3 p_i^2, \quad \forall (p_1, p_2, p_3) \in \mathbb{R}^3, \quad (1.8)$$

with Pauli matrices

$$\sigma_1 = \begin{bmatrix} 0 & 1 \\ 1 & 0 \end{bmatrix}, \quad \sigma_2 = \begin{bmatrix} 0 & -i \\ i & 0 \end{bmatrix}, \quad \sigma_3 = \begin{bmatrix} 1 & 0 \\ 0 & -1 \end{bmatrix}. \quad (1.9)$$

The Pauli matrices look like candidates for matrices in Equation (1.4). However, there are only three linearly independent such matrices for $\alpha_i, i = 1, 2, 3$ and is no more such anti-commuting matrix for β . Dirac decided to enlarge the size of those square matrices. According to (1.5)-(1.7) the matrices α_i and β have eigenvalues ± 1 with 0 matrix trace. Thus, the dimension of such square matrices should be an even number. He enlarged the size from 2×2 to 4×4 and defined

$$\beta = \begin{bmatrix} I_2 & \mathbf{0} \\ \mathbf{0} & -I_2 \end{bmatrix}, \quad \alpha_i = \begin{bmatrix} \mathbf{0} & \sigma_i \\ \sigma_i & \mathbf{0} \end{bmatrix}, \quad i = 1, 2, 3. \quad (1.10)$$

Combining with (1.3) and (1.4) one can get the Dirac equation

$$i\frac{\partial}{\partial t}\psi = (-i\boldsymbol{\alpha} \cdot \nabla + \beta m)\psi \equiv D_m\psi \quad (1.11)$$

where $\psi(x, t) : \mathbb{R}^3 \times \mathbb{R} \rightarrow \mathbb{C}^4$ is the wave function and D_m is called the **Dirac operator**. The matrices $\alpha_1, \alpha_2, \alpha_3$ and β are called *Dirac matrices*. They are Hermitian and thus the operators introduced by (1.4) is self-adjoint. Although the Dirac operator is originally defined in \mathbb{R}^3 , we can generalize the definition in any \mathbb{R}^n where $n \geq 1$ and the size of the corresponding Dirac matrices and the wave function ψ depends on n (see [4]). For example, in \mathbb{R} the Dirac operator can be written as

$$D_m\psi = -i(-\sigma_2\partial_x)\psi + \sigma_3m\psi, \quad \psi : \mathbb{R} \times \mathbb{R}^+ \rightarrow \mathbb{C}^2, \quad (1.12)$$

and in \mathbb{R}^2 the Dirac operator can be written as

$$D_m\psi = -i(\sigma_1\partial_1 + \sigma_2\partial_2)\psi + \sigma_3m\psi, \quad \psi : \mathbb{R}^2 \times \mathbb{R}^+ \rightarrow \mathbb{C}^2, \quad (1.13)$$

where $\sigma_i, i = 1, 2, 3$, are Pauli matrices defined as above. The Dirac operator can also be defined by Clifford multiplication (see [4]).

Remark 1.1.1. *The operator D_m contains the value m which is interpreted as the mass. Throughout the paper, we take $m = 1$. In some contexts, the mass of a particle may be ignored and the corresponding operator is defined as*

$$D_0 = -i\boldsymbol{\alpha} \cdot \nabla. \quad (1.14)$$

It is called massless Dirac operator and has the property

$$D_0^2 = -\Delta I_4, \quad (1.15)$$

where I_4 is the identity matrix. For D_m we have a similar relation

$$D_m^2 = (-\Delta + m^2)I_4. \quad (1.16)$$

1.2 Nonlinear Dirac Equation

In this section, we introduce two types of nonlinear Dirac equations. One model is the NLD with the scalar self-interaction and the other model is the NLD with the Coulomb type nonlinearity.

In 1938, Ivanenko [5] first studied the NLD with scalar self-interaction. The nonlinear self-interaction of the spinor fields may arise due to the geometrical structure of the spacetime [6]. Ivanenko demonstrated a relativistic theory with a fourth order self-interaction. In [7, 8], the authors attempted to formulate a unified theory of elementary particles by using the NLD model. In 1958, Thirring [9] introduced a completely integrable one-dimensional model, known as the Massive Thirring Model, which is based on spinor field with the vector self-interaction. It is notable that fundamental solutions of the MTM can be transformed into solitary wave solutions of the sine-Gordon equation by means of a bosonization process [10]. In 1970, Soler [11] studied Ivanenko's model in the context of extended nucleons and provided the numerical analysis of particle-like-solutions (solitary wave solutions). Nowadays the NLD with scalar self-interaction is called Soler model canonically. The one-dimensional Soler model, also known as the Gross-Neveu model, was introduced in [12] as a toy model of quark confinement. The explicit solutions were given in [13].

The Soler model is written as

$$i\partial_t\psi = D_m\psi - f(\psi^*\beta\psi)\beta\psi, \quad \psi(x, t) \in \mathbb{C}^N, \quad x \in \mathbb{R}^n, \quad t \geq 0, \quad n \geq 1 \quad (1.17)$$

with the real-valued $f(s) = s^k$, $k \in \mathbb{N}$. We note that the equation (1.17) is $U(1)$ -invariant and Hamiltonian, with the corresponding Hamiltonian represented by the density

$$\mathbf{H}(\psi) = \psi^* D_m \psi - F(\psi^* \beta \psi), \quad F(s) = \int_0^s f(r) dt. \quad (1.18)$$

Moreover, the system is also $\text{SU}(1, 1)$ -invariant and Lorentz-invariant. Due to the term $\psi^* D_m \psi$, the functional \mathbf{H} is unbounded from below and sign-indefinite. The fact leads to barriers for the stability analysis, especially comparing to its non-relativistic analogue, the NLS.

Another type of nonlinear Dirac equation is defined with the Coulomb type nonlinearity

$$i\partial_t \psi = D_m \psi + q\Phi\psi, \quad \Delta\Phi = -\psi^* \psi \quad (1.19)$$

where q is the charge ($q < 0$ for electron). The Dirac-Coulomb equation is no longer $\text{SU}(1, 1)$ -invariant and Lorentz-invariant. The system is particularly complicated for the stability analysis, even for the 1D model, since the Coulomb potential will create infinitely many eigenvalues for the linearized system, just like in the Hydrogen atom. Instead, we will consider a toy model

$$i\partial_t \psi = D_m \psi - V\psi, \quad \psi : \mathbb{R} \times \mathbb{R}^+ \rightarrow \mathbb{C}^2. \quad (1.20)$$

where the nonlinearity term V is defined as $V = |\psi|^2$. It is notable that Equation (1.20) is not $\text{SU}(1, 1)$ -invariant as well (the detail will be presented in Section 4.3) and thus it could be considered as a simplified analogue of the 1D Dirac-Coulomb equation.

1.3 Solitary Waves

Solitary waves are localized traveling waves and are well-known in many nonlinear dispersive equations, such as the NLS, the nonlinear sine-Gordon equation and the Korteweg-de Vries equation [14, 15]. The phenomenon of solitary waves was first investigated by J. Scott Russell in 1834. Nowadays the phenomena have been simulated and observed in many physical fields, for instance, the non-linear optics, plasma physics and lattice dynamics.

We will consider solitary wave solutions to the NLD system (1.17):

$$\psi(x, t) = \varphi_\omega(x) e^{-i\omega t}. \quad (1.21)$$

The profile function $\varphi_\omega(x)$ merely depends on spatial variable, so the ‘‘shape’’ of the solution will

not change as it evolves.

By using polar coordinates (the details will be presented later), we can assume that the solitary wave solution is of the form

$$\psi(x, t) = \varphi_\omega(r, \theta, \phi) e^{-i\omega t} = \begin{bmatrix} v(r) \begin{bmatrix} 1 \\ 0 \end{bmatrix} \\ iu(r) \begin{bmatrix} \cos \theta \\ e^{i\phi} \sin \theta \end{bmatrix} \end{bmatrix} e^{-i\omega t}, \quad (1.22)$$

where u and v are both real-valued functions and $\omega \in (0, m)$. After the substitution, Equation (1.17) can be reduced to an ODE system

$$\begin{cases} v'(r) = -(m - f(v^2 - u^2) + \omega)u(r) \\ u'(r) + \frac{2}{r}u(r) = -(m - f(v^2 - u^2) - \omega)v(r) \end{cases}. \quad (1.23)$$

We note the absence of the term $e^{-i\omega t}$, which is canceled out due to the $\mathbf{U}(1)$ -symmetry, and the angular coordinates, so the system is real-valued and merely depends on the radial coordinate r . Usage of the solitary wave Ansatz (1.22) substantially simplifies the original equation (1.17) and leads to tremendous simplification for the analyses and numerics.

To eliminate the singularity resulted from the term $\frac{2}{r}u(r)$, we assume that $u(0) = 0$. Since the solitary wave solutions correspond to extended Fermions [11, 6], u, v, u' and v' have to vanish at infinity. The existence of such u and v has been proved in different approaches. In [16], the authors use a shooting method to show the existence of u and v , which are in \mathcal{C}^1 and decay exponentially at infinity, under the following hypotheses on f :

1. $f : [0, +\infty] \rightarrow [0, +\infty]$ in \mathcal{C}^1 ;
2. $f(0) = 0, f'(r) > 0$ for $r > 0$;
3. $\lim_{r \rightarrow +\infty} f(r) = +\infty$.

Obviously, $f(s) = s^k$, $k \in \mathbb{N}$ satisfies all the conditions above. In [17], the author also uses a shooting method to show the existence without the assumption that f is increasing on $(0, +\infty)$. In [18], the authors use a variational approach to show the existence. The hypotheses on f are similar to the ones in [16] and the only difference is that authors assume that $rf(r) > \epsilon F(r)$ for $\epsilon > 1$, $r > 0$, where F is the anti-derivative of f with $F(0) = 0$, instead of f being increasing. The setting $f(s) = s^k$, $k \in \mathbb{Z}_+$, also satisfies the assumption.

In the case of $x \in \mathbb{R}^2$, we have the similar format for the solitary waves

$$\psi(x, t) = \varphi_\omega(r, \theta)e^{-i\omega t} = \begin{bmatrix} v(r) \\ iu(r)e^{i\theta} \end{bmatrix} e^{-i\omega t}, \quad (1.24)$$

and the corresponding ODE system is

$$\begin{cases} v'(r) = -(m - f(v^2 - u^2) + \omega)u(r) \\ u'(r) + \frac{1}{r}u(r) = -(m - f(v^2 - u^2) - \omega)v(r) \end{cases}. \quad (1.25)$$

The only difference is the coefficient at the singular term $u(r)/r$. The existence can be shown by the same approaches as in the 3D case.

In the case of $x \in \mathbb{R}$, the solitary wave is of the form

$$\psi(x, t) = \varphi_\omega(r, \theta)e^{-i\omega t} = \begin{bmatrix} v(r) \\ u(r) \end{bmatrix} e^{-i\omega t}, \quad (1.26)$$

and the corresponding system ODE system is

$$\begin{cases} v'(r) = -(m - f(v^2 - u^2) + \omega)u(r) \\ u'(r) = -(m - f(v^2 - u^2) - \omega)v(r) \end{cases}. \quad (1.27)$$

The term $u(r)/r$ disappears and the existence of u and v is proved by constructing a Hamiltonian

system corresponding to (1.27) in [19].

For Equation (1.20), we take the solitary waves as

$$\psi = \varphi_\omega(x)e^{-i\omega t}, \quad \varphi_\omega(x) = \begin{bmatrix} v(x) \\ u(x) \end{bmatrix}, \quad (1.28)$$

where u and v are also real-valued functions and the ODE system is written as

$$\begin{cases} \omega v = u' + mv - (u^2 + v^2)v, \\ \omega u = -v' - mu - (u^2 + v^2)u. \end{cases} \quad (1.29)$$

The existence of solutions to Equation (1.29) will be shown in our work.

1.4 Stability Analysis

The stability of a particular solution to a PDE system is a crucial property. Roughly, a solution to some system is called stable if another solution with initial data near the initial value of that solution will keep close to that solution for all times. For different systems, different types of norms may be applied, say L^2 -norm or H^2 -norm, to describe how close those two solutions are. The stability is important because an unstable solution cannot be implemented in the physical and industrial contexts. For most PDEs, especially nonlinear systems, analytical solutions cannot be obtained explicitly and thus the numerical solutions play important roles. However, the numerical solution would be meaningless if the solution were unstable, since numerical errors cannot be avoided during numerical computations. According to the complexity and accessibility of a system, we will investigate distinct types of stability.

Let us first recall some basic definitions in the spectral theory. Suppose that \mathcal{H} is a Hilbert space and $A \in \mathcal{L}(\mathcal{H})$ is a linear operator in \mathcal{H} with domain $\mathfrak{D}(A)$.

Definition 1.4.1. *A is called **closed** if for any sequence $x_n \in \mathfrak{D}(A)$ such that $x_n \rightarrow x$ and $Ax_n \rightarrow y$ as $n \rightarrow \infty$, it follows that $x \in \mathfrak{D}(A)$ and $Ax = y$. A is called **densely defined operator** if $\mathfrak{D}(A)$ is dense in \mathcal{H} .*

We assume that all the linear operators are closed and densely defined throughout the paper.

Remark 1.4.1. *Since A is closed, if $A - \lambda I_{\mathcal{H}}$ is a bijection, then $(A - \lambda I_{\mathcal{H}})$ is a bounded operator by the closed graph theorem.*

Definition 1.4.2 (Resolvent set). *The **resolvent set** $\rho(A)$ is the set of all $\lambda \in \mathbb{C}$ such that the map $(A - \lambda I_{\mathcal{H}}) : \mathfrak{D}(A) \rightarrow \mathcal{H}$ is bijective. If $\lambda \in \rho(A)$, then the corresponding resolvent operator is defined as $(A - \lambda I_{\mathcal{H}})^{-1}$.*

Definition 1.4.3 (Spectrum). *The set $\sigma(A) = \mathbb{C} \setminus \rho(A)$ is called the **spectrum** of A . In other words, if $\lambda \in \sigma(A)$, then $(A - \lambda I_{\mathcal{H}})$ does not have the inverse.*

Definition 1.4.4 (Eigenvalue). *A complex number λ is called an **eigenvalue** of A , if there exist a nonzero $f \in \mathfrak{D}(A)$ such that $\lambda f = Af$. In other words, $(A - \lambda I_{\mathcal{H}})$ has a nontrivial null space in \mathcal{H} . And f is called the **eigenvector** or **eigenfunction** associated with the eigenvalue λ . The null space of $(A - \lambda I_{\mathcal{H}})$ is called the eigenspace associated with λ and the dimension of the null space is called the **geometric multiplicity** of λ .*

In the physical contexts, \mathcal{H} is usually a space equipped with the energy norm, for instance, L^2 or H^1 and thus the desired eigenfunctions have to decay sufficiently fast at infinity.

There are several specific spectra.

Definition 1.4.5 (Point Spectrum). *The **point spectrum** $\sigma_p(A)$ is the set of all the eigenvalues.*

Definition 1.4.6 (Discrete Spectrum). *The **discrete spectrum** $\sigma_d(A)$ is set of all the isolated eigenvalues such that the corresponding Riesz projector has a finite rank.*

Definition 1.4.7 (Essential Spectrum). *The **essential spectrum** $\sigma_{\text{ess}}(A)$ is defined as the set $\sigma(A) \setminus \sigma_d(A)$.*

Remark 1.4.2. *There are various definitions of the essential spectrum, which are not equivalent (see [20]). The definition above agrees with $\sigma_{\text{ess},5}(A)$ in [20].*

Since eigenvalues may be embedded in the essential spectrum and there could be an isolated eigenvalues of infinite algebraic multiplicity, $\sigma_p(A)$ and $\sigma_d(A)$ are not equivalent.

Now we will introduce several types of stability for the solutions to NLDs. We are interested in the solitary wave solution (1.21), namely $\psi(x, t) = \varphi(x)e^{-i\omega t}$, to systems (1.17) and (1.20). Consider a perturbation of the solitary wave of the form

$$\psi(x, t) = (\varphi_\omega(x) + R(x, t))e^{-i\omega t}. \quad (1.30)$$

We substitute (1.21) by perturbation (1.30) in the Systems (1.17) and (1.20) and linearize the systems with respect to the term $R(x, t)$. The linearized form is given by

$$\partial_t R = \mathcal{L}R + o(R) \quad (1.31)$$

where \mathcal{L} is the linearization operator corresponding to the original systems.

Definition 1.4.8 (Spectral Stability). *If $\sigma_p(A)$ lies entirely on the left-half plane (including the imaginary axis), then the solitary wave (1.21) is called **spectrally stable**. Otherwise, the solitary wave (1.21) is called **linearly unstable**.*

Definition 1.4.9 (Orbital Stability). *The solitary wave (1.21) is called **orbitally stable** if for any $\epsilon > 0$ there is $\delta > 0$ such that if $\|\phi(x, 0) - \psi(x, 0)\| < \delta$ in a certain energy norm (usually L^2 or H^1), then there is a solution $\phi(x, t)$ which exists for all $t \geq 0$ and satisfies $\sup_{t \geq 0} \inf_{s \in \mathbf{R}} \|\phi - e^{is}\psi\| < \epsilon$. Otherwise, the solitary wave is called **orbitally unstable**.*

The orbital stability is introduced in [21] to study the abstract Hamiltonian system. A solitary wave is called orbitally stable if any solution which is sufficiently close to it initially (at $t = 0$) will always keep close to the orbit spanned by the solitary wave.

Definition 1.4.10. *The solitary wave (1.21) is called **asymptotically stable** if any solution initially close to it will converge (in a certain norm) to this or to a nearby solitary wave solution.*

In last decades, many results for different types of stability have been obtained for NLS, Korteweg-de Vries, Klein-Gordon and sine-Gordon equations, see e.g. [22, 23, 24, 25, 26, 21, 27, 28, 29, 30, 31, 32, 33], but the research on the NLD progresses slowly. One important reason is that the Hamiltonian functions corresponding to those models are of finite Morse indices. Hence the solitary waves can be deduced as the minimizer of the energy under some constraints [21]. However, for the NLD, the Hamiltonian is sign indefinite and is of infinite Morse index at the points of the functional space corresponding to solitary waves. As a result, the conservation laws are not sufficient to control all the directions of the perturbation and the methods used to study NLS may not work anymore. We need to find a new approach to show the orbital and asymptotic stability.

In [34, 27], the spectral stability of solitary waves was first studied for a scalar NLS. A priori, the spectral stability leads to neither the orbital stability nor the asymptotic stability. However, according to the results on NLS and Klein-Gordon equations in [27, 35], the linear instability leads to the orbital instability. Meanwhile, the results on asymptotic stability of solitary waves for some NLDs are presented in [36, 37, 38] with some specific restrictions on the spectrum of the linearized operator and sometimes on the structure of allowed perturbations. Thus, we expect that spectral stability is a necessary condition for orbital and asymptotic stability for the system with sign-indefinite Hamiltonian such as NLD. There is an exceptional case, a 1D NLD called the massive Thirring model, which is written as a system of two semi-linear equations in the normalized form:

$$\begin{cases} i(u_t + u_x) + v = 2|v|^2u, \\ i(v_t - v_x) + u = 2|u|^2v, \end{cases} \quad (1.32)$$

where $u(x, t), v(x, t) : \mathbb{R} \times \mathbb{R}_+ \rightarrow \mathbb{C}^2$. This system is completely integrable and some additional conserved quantities arise from the integrability. Due to those conserved quantities, the solitary wave solutions to the 1D MTM system are shown to be orbitally stable in the norm of L^2 and H^1 in [39, 40], respectively.

2. 2D SOLER MODEL*

2.1 The Model

In this chapter, we consider the 2D Soler model, which is written as

$$i\partial_t\psi = D_m\psi - f(\psi^*\beta\psi)\beta\psi, \quad \psi(x, t) \in \mathbb{C}^2, \quad x \in \mathbb{R}^2, \quad t \geq 0, \quad n \geq 1 \quad (2.1)$$

where $D_m = -i\alpha_1\partial_1 - i\alpha_2\partial_2 + \beta m$, $f(s) = s^k$, $k \in \mathbb{N}$, and we use the Pauli matrices σ_j , $1 \leq j \leq 3$, as the Dirac matrices:

$$\alpha_1 = \sigma_1 = \begin{bmatrix} 0 & 1 \\ 1 & 0 \end{bmatrix}, \quad \alpha_2 = \sigma_2 = \begin{bmatrix} 0 & -i \\ i & 0 \end{bmatrix}, \quad \beta = \sigma_3 = \begin{bmatrix} 1 & 0 \\ 0 & -1 \end{bmatrix}. \quad (2.2)$$

The corresponding Lagrangian density is written as

$$\mathcal{L} = \psi^*\beta(i\partial_t - D_m)\psi + F(\psi^*\beta\psi)\psi, \quad (2.3)$$

with $F(s) = s^{k+1}/(k+1)$, the anti-derivative of $f(s)$. The nonlinearity term is called scalar self-interaction, which means that the Lagrangian is based on the term $\psi^*\beta\psi$ and transforms as the scalar under the Lorentz transformations.

For computational convenience, we use the polar coordinates (r, θ) defined as

$$x_1 = r \cos \theta, \quad x_2 = r \sin \theta, \quad (2.4)$$

*Part of this chapter is reprinted with permission from "Stability of Solitary Waves and Vortices in a 2D Nonlinear Dirac Model," J. Cuevas-Maraver, P. G. Kevrekidis, A. Saxena, A. Comech, and R. Lan, 2016. Physical Review Letters, 116, 214101, Copyright [2016] American Physical Society.

and then D_m takes the form

$$D_m = -i\boldsymbol{\alpha} \cdot \nabla + \beta m = \begin{bmatrix} m & -ie^{-i\theta}(\partial_r - \frac{i}{r}\partial_\theta) \\ -ie^{i\theta}(\partial_r + \frac{i}{r}\partial_\theta) & -m \end{bmatrix}. \quad (2.5)$$

As mentioned before, we consider the solitary waves $\psi(x, t) = \varphi_\omega(x)e^{-i\omega t}$ with the profile φ_ω of the form

$$\varphi_\omega(x) = \begin{bmatrix} v(r) \\ iu(r)e^{i\theta} \end{bmatrix} \quad (2.6)$$

where u and v are both real-valued functions. After substituting, we obtain an ODE system with respect to u and v :

$$\begin{cases} v'(r) = -(m - f(v^2 - u^2) + \omega)u(r) \\ u'(r) + \frac{1}{r}u(r) = -(m - f(v^2 - u^2) - \omega)v(r) \end{cases}. \quad (2.7)$$

Remark 2.1.1. *We always assume that the function φ_ω depends on ω , although sometimes we will drop the subscript. Here and throughout the paper we consider the solitary waves for $\omega \in (0, m)$ and φ stands for φ_ω for short unless stated otherwise.*

The system only depends on the radial coordinate r and the existence of solutions has been shown in [16, 17, 18]. The solutions u and v are in C^1 and decay exponentially at infinity. Also $u(0) = 0$ is required because of the term $\frac{1}{r}u(r)$ in the second equation. Even though the existence of such solutions have been shown in many different ways, no explicit solutions have been found by now. Therefore, we have to solve the system numerically. We list the properties for numerical solutions u and v :

1. $u(0) = 0$ and $v(0) > 0$;
2. $u(r)$ and $v(r)$ are nonnegative for $r > 0$;
3. u and v decay quite rapidly at infinity;

4. u' and v' are negative when $r \gg 1$.

Usually we need to know the initial value to solve an ODE system. But for this case, the value of $v(0)$ is unknown, so shooting method is perfectly suitable for this problem. We can set the initial value of v first, and then adjust that value according to Properties 2-4. From Figure 2.1, we can observe that the numerical solutions satisfy all properties above. If we extend r to the domain $(-\infty, +\infty)$, then both v and u extend to C^1 -functions on \mathbb{R} which are even and odd, respectively.

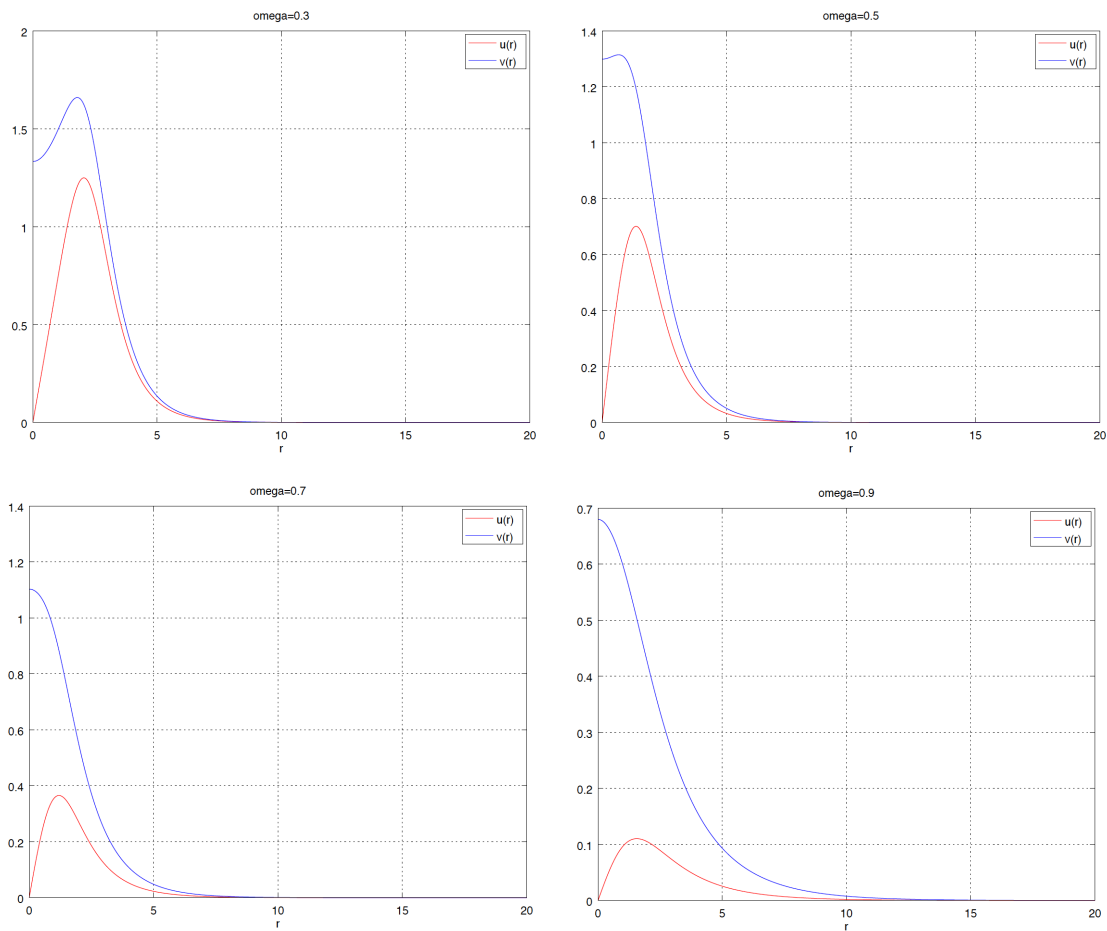


Figure 2.1: Numerical solutions u and v for different values of ω in the 2D Soler model. Here we set $m = 1$ and $f(s) = s$.

The solitary wave (2.6) has been shown to be a stationary solution to Equation (2.1) in many

papers [16, 17, 41, 18], but there are few results concerning the stability of this solitary wave. We will focus on spectral stability of the solitary wave solutions to the 2D Soler model.

2.2 Linearization

To explore the spectral stability, we need to linearize Equation (2.1). We consider a solitary wave with a perturbation in the form of $(\varphi(x) + R(x, t))e^{-i\omega t}$, where $\varphi(x)e^{-i\omega t}$ is a solitary wave solution and $\varphi(x)$ is defined by Equation (2.6). To linearize equation with respect to the perturbation R , we plug the solitary wave with perturbation into Equation (2.1). After eliminating some terms according to Equation (2.1) and ignoring nonlinear terms containing R , we obtain the linearized equation

$$i\partial_t R = D_m R - \omega R - f\beta R - 2\text{Re}(\varphi^* \beta R) f' \beta \varphi, \quad (2.8)$$

where $f = f(\varphi^* \beta \varphi)$ and $f' = f'(\varphi^* \beta \varphi)$, namely, $f = f(v^2 - u^2)$ and $f' = f'(v^2 - u^2)$. Since we explore the spectral stability and deal with eigenfunctions, the perturbation should be sufficiently smooth. We have the following lemma.

Lemma 2.2.1. *Assume that the solitary wave profile φ belongs to $H^1(\mathbb{R}^2, \mathbb{C}^2)$ and $f(s) = s^k$, $k \in \mathbb{N}$. If $R \in L^2(\mathbb{R}^2, \mathbb{C}^2)$ is an eigenfunction of the linear operator \mathcal{L} defined by*

$$\mathcal{L}_2 R = D_m R - \omega R - f\beta R - 2\text{Re}(\varphi^* \beta R) f' \beta \varphi \quad (2.9)$$

corresponding to the eigenvalue $\lambda \in \mathbb{C}$, then $R \in H^2(\mathbb{R}^2, \mathbb{C}^2)$.

Proof. Since R is an eigenfunction associated with the eigenvalue λ , we have

$$\lambda R = D_0 R + \beta m R - \omega R - f\beta R - 2\text{Re}(\varphi^* \beta R) f' \beta \varphi.$$

It implies that

$$D_0 R = \lambda R - \beta m R + \omega R + f\beta R + 2\text{Re}(\varphi^* \beta R) f' \beta \varphi. \quad (2.10)$$

Since $\varphi \in H^1(\mathbb{R}^2, \mathbb{C}^4)$ with u and v decaying exponentially at infinity, both f and f' are in

$H^1(\mathbb{R}^2, \mathbb{C}^4)$ as well. We know that all the terms on the right hand side in Equation (2.10) are in $L^2(\mathbb{R}^2, \mathbb{C}^2)$. It follows that $D_0 R \in L^2(\mathbb{R}^2, \mathbb{C}^2)$ and thus $R \in H^1(\mathbb{R}^2, \mathbb{C}^4)$. Now applying the operator D_0 on both side of Equation (2.10) and due to Equation (1.15) we have

$$-\Delta R = \lambda D_0 R - \beta m D_0 R + \omega D_0 R + D_0(f\beta R + 2\text{Re}(\varphi^* \beta R) f' \beta \varphi). \quad (2.11)$$

Obviously, all the terms on the right hand side are in $L^2(\mathbb{R}^2, \mathbb{C}^2)$ since u and v are differentiable and decay exponentially at infinity. It follows that $\Delta R \in L^2(\mathbb{R}^2, \mathbb{C}^2)$ and thus $R \in H^2(\mathbb{R}^2, \mathbb{C}^2)$. \square

We should investigate the point spectrum of the linear operator \mathcal{L}_2 defined in Equation (2.9) to examine the spectral stability. However, $\mathcal{L}_2 R$ contains the term $2\text{Re}(\varphi^* \beta R) f' \beta \varphi$, which makes the operator only \mathbb{R} -linear, but not \mathbb{C} -linear. To conquer this barrier, we complexify the operator by separating the real parts and imaginary parts for each components in R . For computational convenience, we choose R in the form similar to the profile function (2.6) and it is written as

$$R = \begin{bmatrix} R_1 + iS_1 \\ e^{i\theta}(R_2 + iS_2) \end{bmatrix} \quad (2.12)$$

where $R_i(r, \theta, t), S_i(r, \theta, t), i = 1, 2$, are real-valued functions. By taking R in the form (2.12), Equation (2.8) turn into

$$i\partial_t \begin{bmatrix} R_1 + iS_1 \\ e^{i\theta}(R_2 + iS_2) \end{bmatrix} = (D_m - \omega - f\beta) \begin{bmatrix} R_1 + iS_1 \\ e^{i\theta}(R_2 + iS_2) \end{bmatrix} - 2(vR_1 - uS_2) f' \beta \varphi.$$

Using the polar coordinates and writing D_m explicitly, we have

$$i\partial_t \begin{bmatrix} R_1 + iS_1 \\ e^{i\theta}(R_2 + iS_2) \end{bmatrix} = \begin{bmatrix} m - \omega - f & -e^{-i\theta}(i\partial_r + \frac{1}{r}\partial_\theta) \\ -e^{i\theta}(i\partial_r - \frac{1}{r}\partial_\theta) & -m - \omega + f \end{bmatrix} \begin{bmatrix} R_1 + iS_1 \\ e^{i\theta}(R_2 + iS_2) \end{bmatrix} - 2(vR_1 - uS_2)f' \begin{bmatrix} v \\ -iue^{i\theta} \end{bmatrix}.$$

By observation, we note that only the second row contain the multiplier $e^{i\theta}$, so we can cancel that term and we obtain the system

$$i\partial_t \begin{bmatrix} R_1 + iS_1 \\ R_2 + iS_2 \end{bmatrix} = \begin{bmatrix} m - \omega - f & -(i\partial_r + \frac{i}{r} + \frac{1}{r}\partial_\theta) \\ -(i\partial_r - \frac{1}{r}\partial_\theta) & -m - \omega + f \end{bmatrix} \begin{bmatrix} R_1 + iS_1 \\ (R_2 + iS_2) \end{bmatrix} - 2(vR_1 - uS_2)f' \begin{bmatrix} v \\ -iu \end{bmatrix}.$$

Now we collect real parts and imaginary parts in separate systems. In this way, the constant i can be eliminated and equations can be simplified. For S_1 and S_2 we have

$$-\partial_t \begin{bmatrix} S_1 \\ S_2 \end{bmatrix} = \begin{bmatrix} (m - \omega - f)R_1 - (-\partial_r S_2 - \frac{1}{r}S_2 + \frac{1}{r}\partial_\theta R_2) \\ -(-\partial_r S_1 - \frac{1}{r}\partial_\theta R_1) + (-m - \omega + f)R_2 \end{bmatrix} - 2(vR_1 - uS_2)f' \begin{bmatrix} v \\ 0 \end{bmatrix},$$

and for R_1 and R_2 we have

$$\partial_t \begin{bmatrix} R_1 \\ R_2 \end{bmatrix} = \begin{bmatrix} (m - \omega - f)S_1 - (\partial_r + \frac{1}{r})R_2 - \frac{1}{r}\partial_\theta S_2 \\ -(\partial_r R_1 - \frac{1}{r}\partial_\theta S_1) + (-m - \omega + f)S_2 \end{bmatrix} - 2(vR_1 - uS_2)f' \begin{bmatrix} 0 \\ -u \end{bmatrix}.$$

After re-arrangement we obtain

$$\partial_t \begin{bmatrix} S_1 \\ S_2 \end{bmatrix} = \begin{bmatrix} (-m + \omega + 2v^2 f' + f)R_1 + \frac{1}{r}\partial_\theta R_2 + (-2uvf' - \partial_r - \frac{1}{r})S_2 \\ (-\frac{1}{r}\partial_\theta R_1) + (m + \omega - f)R_2 - \partial_r S_1 \end{bmatrix},$$

and

$$\partial_t \begin{bmatrix} R_1 \\ R_2 \end{bmatrix} = \begin{bmatrix} (m - \omega - f)S_1 - (\partial_r + \frac{1}{r})R_2 - \frac{1}{r}\partial_\theta S_2 \\ (2uvf' - \partial_r)R_1 + \frac{1}{r}\partial_\theta S_1 + (-m - \omega + f - 2u^2f')S_2 \end{bmatrix}.$$

We combine them together and obtain the following system:

$$\partial_t \begin{bmatrix} R_1 \\ S_1 \\ R_2 \\ S_2 \end{bmatrix} = \mathcal{A} \begin{bmatrix} R_1 \\ S_1 \\ R_2 \\ S_2 \end{bmatrix}, \quad (2.13)$$

where \mathcal{A} is a matrix operator from $H^1(\mathbb{R}^2, \mathbb{C}^4)$ to $L^2(\mathbb{R}^2, \mathbb{C}^4)$ and is written as

$$\mathcal{A} = \begin{bmatrix} 0 & m - \omega - f & -\partial_r - \frac{1}{r} & -\frac{\partial_\theta}{r} \\ \omega - m + 2v^2f' + f & 0 & \frac{\partial_\theta}{r} & -2uvf' - \partial_r - \frac{1}{r} \\ 2uvf' - \partial_r & \frac{\partial_\theta}{r} & 0 & -m - \omega + f - 2u^2f' \\ -\frac{\partial_\theta}{r} & -\partial_r & m + \omega - f & 0 \end{bmatrix}.$$

Remark 2.2.1. *The operator \mathcal{A} depends on the frequency parameter ω .*

It suffices to compute the point spectrum of the operator \mathcal{A} :

$$\sigma_p(\mathcal{A}) = \{\lambda \in \mathbb{C}; \quad \lambda\Psi = \mathcal{A}\Psi, \quad \Psi \in L^2(\mathbb{R}^2, \mathbb{C}^4), \quad \Psi \neq 0\}$$

to determine the spectral stability.

2.3 Evans Function and Jost Solution

In order to compute the $\sigma_p(\mathcal{A})$ we can apply the Evans function which provides an efficient tool to locate the eigenvalue values for a linear differential operator.

2.3.1 Introduction

The Evans function was first introduced by J.W. Evans [42, 43, 44, 45] in his study of the stability of nerve impulses. Evans defined $\mathfrak{D}(\lambda)$ to represent the determinant for eigenvalue problems associated with traveling waves of a class of nerve impulse models. $\mathfrak{D}(\lambda)$ was constructed to detect the intersections of the subspaces of solutions decaying exponentially to the positive infinity and the negative infinity, respectively. Since the class of equations in his study has some special property, the construction for $D(\lambda)$ is straightforward. In [46], Jones implemented Evans' idea to study the stability of a singularly perturbed FitzHugh-Nagumo system and called the determinant-like function the Evans function. In his paper, $E(\lambda)$ is used to denote the Evans function, which has become the canonical notation. The first general definition of the Evans function was given in [47] and the authors study the stability for traveling waves of a semi-linear parabolic system. Pego and Weinstein [48] expanded on Jones' construction of the Evans function to study the linear instability of solitary waves in the Korteweg-de Vries equation, the Benjamin-Bona-Mahoney equation and the Boussinesq equation. Generally, the Evans function for a differential operator \mathcal{D} is an analytic function such that $E(\lambda) = 0$ if and only if λ is an eigenvalue of \mathcal{D} , and the order of zero is equal to the algebraic multiplicity of the eigenvalue. Usually the Evans function is defined via the Jost solutions, which are solutions to eigenvalue problems associated with a differential operator and certain boundary conditions at $\pm\infty$. In this way, the corresponding eigenfunctions can be arranged in the space equipped with some specific norm.

2.3.2 A Simple Example

We present a simple example to illustrates how to construct the Evans function. Consider a stationary Schrödinger equation

$$-\kappa^2 u(x) = Hu(x) \quad u(x) \in \mathbb{C}, \quad x \in \mathbb{R}, \quad (2.14)$$

where $H = -\partial_x^2 + V$ with a potential $V \in C(\mathbb{R})$, $\text{supp } V \subset [-1, 1]$. For $\kappa \in \mathbb{C} \setminus \{0\}$, $\text{Re } \kappa > 0$, it has solutions $J_+(\kappa, x)$ and $J_-(\kappa, x)$ in $H^2(\mathbb{C})$, defined by their behavior at $\pm\infty$:

$$J_+(\kappa, x) = e^{-\kappa x}, \quad x \geq 1; \quad J_-(\kappa, x) = e^{+\kappa x}, \quad x \leq -1.$$

We note that J_+ and J_- decay exponentially as $x \rightarrow \pm\infty$, respectively, since $\text{Re } \lambda > 0$. J_+ and J_- are called Jost solutions to (2.14) and the Evans function is constructed by the Wronskian of J_+ and J_- :

$$E(\kappa) = W(J_+, J_-)(x, \kappa), \quad (2.15)$$

where

$$W(J_+, J_-)(x, \kappa) = \det \begin{bmatrix} J_+ & J_- \\ \partial_x J_+ & \partial_x J_- \end{bmatrix} = J_+(x, \kappa) \partial_x J_-(x, \kappa) - J_-(x, \kappa) \partial_x J_+(x, \kappa). \quad (2.16)$$

To make $E(\kappa)$ well-defined, we need to show that the Wronskian only depends on κ .

Lemma 2.3.1. *The Wronskian $W(J_+, J_-)(x, \kappa)$ defined by Equation (2.16) does not depend on x .*

Proof. Differentiate Equation (2.16) with respect to x

$$\partial_x W(J_+, J_-)(x, \kappa) = J_+(x, \kappa) \partial_x^2 J_-(x, \kappa) - J_-(x, \kappa) \partial_x^2 J_+(x, \kappa).$$

Since both J_+ and J_- are both solutions to Equation (2.14), we have

$$\partial_x^2 J_+(x, \kappa) = \kappa^2 J_+(x, \kappa) + V(x) J_+(x, \kappa), \quad \partial_x^2 J_-(x, \kappa) = \kappa^2 J_-(x, \kappa) + V(x) J_-(x, \kappa).$$

It follows that $\partial_x W(J_+, J_-)(x, \kappa) = 0$ and thus $W(J_+, J_-)(x, \kappa)$ does not depend on x . \square

If $E(\kappa)$ vanishes at some particular $\lambda \in \mathbb{C}$ with $\text{Re } \lambda > 0$, the Jost solutions J_+ and J_- are linearly dependent; in other words, there exists $c \in \mathbb{C} \setminus \{0\}$ such that $J_+(x, \kappa) = c J_-(x, \kappa)$ for

$x \in \mathbb{R}$. We can define an eigenfunction as

$$\varphi(x) = \begin{cases} J_+(x, \kappa), & x \geq 0 \\ cJ_-(x, \kappa), & x < 0 \end{cases}$$

which is in $H^2(\mathbb{C})$ and thus it is an eigenfunction corresponding to an eigenvalue $\lambda = -\kappa^2$ of the Schrödinger operator H .

2.3.3 1D Soler Model

In [19] the solitary waves for 1D Soler model are shown to be spectrally stable with the aid of the Evans function technique. This was the first definitive spectral stability result in the context of NLD. Since we will apply the same idea to construct Evans functions for 2D and 3D Soler models, we summarize the procedures to construct the Evans function used in that paper.

The authors consider a solitary wave (1.28) for 1D Soler model with cubic nonlinearity

$$i\partial_t \psi = D_m \psi - (\psi^* \beta \psi) \beta \psi, \quad \psi : \mathbb{R} \times \mathbb{R}^+ \rightarrow \mathbb{C}^2, \quad (2.17)$$

where D_m is defined as (1.12). Then the equation is linearized on the perturbation $\psi(x, t) = (\varphi(x) + \rho(x, t))e^{-i\omega t}$ with $\rho \in \mathbb{C}^2$ and the linearized equation is of the form

$$\partial_t R = \mathcal{A}R, \quad (2.18)$$

with $R = [\operatorname{Re}\rho, \operatorname{Im}\rho]^T \in \mathbb{R}^4$ and

$$\mathcal{A} = \begin{bmatrix} 0 & L_0(\omega) \\ -L_1(\omega) & 0 \end{bmatrix}, \quad (2.19)$$

where the operators $L_0(\omega)$ and $L_1(\omega) : L^2(\mathbb{R}^2, \mathbb{C}^2) \rightarrow L^2(\mathbb{R}^2, \mathbb{C}^2)$ with the domain $\mathfrak{D}(L_0) =$

$\mathfrak{D}(L_1) = H^1(\mathbb{R}^2, \mathbb{C}^2)$ are self-adjoint and defined by

$$L_0(\omega) = \begin{pmatrix} m - f - \omega & \partial_x \\ -\partial_x & -m + f - \omega \end{pmatrix},$$

$$L_1(\omega) = L_0(\omega) - 2f' \begin{pmatrix} v^2 & -vu \\ -vu & u^2 \end{pmatrix},$$

with f and f' evaluated at $v^2 - u^2$.

The construction is done by decomposing $L^2(\mathbb{R}, \mathbb{C}^4)$ into two subspaces: the “even” subspace X^\diamond with even first and third components and with odd second and fourth components, and the “odd” subspace X^\bullet with odd first and third components and with even second and fourth components. direct sum of X^\diamond and X^\bullet coincides with $L^2(\mathbb{R}, \mathbb{C}^4)$ and the operator \mathcal{A} introduced in Equation (2.18) acts invariantly on them, all the eigenvalue of \mathcal{A} have corresponding eigenfunctions either in X^\diamond or in X^\bullet , namely,

$$\sigma_p(\mathcal{A}) = \sigma_p(\mathcal{A}|_{X^\diamond}) \cup \sigma_p(\mathcal{A}|_{X^\bullet}). \quad (2.20)$$

Thus, the Evans function can be constructed in X^\diamond and X^\bullet separately.

The Evans functions corresponding to X^\diamond and X^\bullet are defined by

$$E_{X^\diamond}(\lambda) = \det(R_1, R_3, J_1, J_2), \quad (2.21)$$

$$E_{X^\bullet}(\lambda) = \det(R_2, R_4, J_1, J_2), \quad (2.22)$$

respectively, where $R_j(x)$, $1 \leq j \leq 4$, are the solutions to the equation $\lambda R = \mathcal{A}R$ with the

following initial data at $x = 0$:

$$R_1|_{x=0} = \begin{bmatrix} 1 \\ 0 \\ 0 \\ 0 \end{bmatrix}, \quad R_2|_{x=0} = \begin{bmatrix} 0 \\ 1 \\ 0 \\ 0 \end{bmatrix}, \quad R_3|_{x=0} = \begin{bmatrix} 0 \\ 0 \\ 1 \\ 0 \end{bmatrix}, \quad R_4|_{x=0} = \begin{bmatrix} 0 \\ 0 \\ 0 \\ 1 \end{bmatrix},$$

and J_1 and J_2 are the Jost solution corresponding to \mathcal{A} , more precisely, they are solutions to $\lambda\Psi = A\Psi$ with the same asymptotics at $+\infty$ as the solutions in $L^2(\mathbb{R}, \mathbb{C}^4)$ to $\lambda\Psi = (\mathbf{D}_m - \omega)\Psi$ with

$$\mathbf{D}_m = \begin{bmatrix} D_m & 0 \\ 0 & D_m \end{bmatrix}.$$

The key step in the process is decomposing $L^2(\mathbb{R}, \mathbb{C}^4)$ into two subspaces which A acts invariantly on. Then Evans functions can be constructed on each subspace separately. We will implement this method for the 2D Soler model to factorize the linearized operator on invariant subspaces.

2.4 Evans function Factorization

Recall the linearized operator introduced in Equation (2.13):

$$\mathcal{A} = \begin{bmatrix} 0 & m - \omega - f & -\partial_r - \frac{1}{r} & -\frac{\partial_\theta}{r} \\ \omega - m + 2v^2 f' + f & 0 & \frac{\partial_\theta}{r} & -2uv f' - \partial_r - \frac{1}{r} \\ 2uv f' - \partial_r & \frac{\partial_\theta}{r} & 0 & -m - \omega + f - 2u^2 f' \\ -\frac{\partial_\theta}{r} & -\partial_r & m + \omega - f & 0 \end{bmatrix}.$$

By observation \mathcal{A} depends explicitly on polar coordinate variable r and the corresponding differential operator ∂_r and ∂_θ , but not on θ . Therefore, we decompose $L^2(\mathbb{R}^2, \mathbb{C}^4)$ by the Fourier

decomposition with respect to θ , namely,

$$\mathcal{X}_l = \left\{ \begin{bmatrix} F_1(r) \\ G_1(r) \\ F_2(r) \\ G_2(r) \end{bmatrix} e^{il\theta}; \quad F_j, G_j \in L^2(\mathbb{R}_+, \mathbb{C}), \quad j = 1, 2 \right\}, \quad l \in \mathbb{Z}. \quad (2.23)$$

Remark 2.4.1. If $\Phi \in \mathcal{X}_l$ is a eigenfunction corresponding to \mathcal{A}_l and is of the form

$$\Phi(r, \theta) = \begin{bmatrix} F_1(r) \\ G_1(r) \\ F_2(r) \\ G_2(r) \end{bmatrix} e^{il\theta}, \quad (2.24)$$

then the functions $F_j, G_j, j = 1, 2$ are in H^2 by Lemma 2.2.1.

Lemma 2.4.1. The operator \mathcal{A} acts invariantly in the subspace \mathcal{X}_l . In other words, for any $\Psi \in \mathcal{X}_l \cap \mathfrak{D}(\mathcal{A})$, one has $\mathcal{A}\Psi \in \mathcal{X}_l$.

Proof. Suppose that $\Phi \in \mathcal{X}_l$ and is written as Equation (2.24). Then we have

$$\mathcal{A}\Phi = \begin{bmatrix} 0 & m - \omega - f & -\partial_r - \frac{1}{r} & -\frac{il}{r} \\ \omega - m + f + 2v^2 f' & 0 & \frac{il}{r} & -2uvf' - \partial_r - \frac{1}{r} \\ 2uvf' - \partial_r & \frac{il}{r} & 0 & -m - \omega + f - 2u^2 f' \\ -\frac{il}{r} & -\partial_r & m + \omega - f & 0 \end{bmatrix} \Phi,$$

and thus

$$\mathcal{A}|_{\mathcal{X}_l} = \begin{bmatrix} 0 & m - \omega - f & -\partial_r - \frac{1}{r} & -\frac{il}{r} \\ \omega - m + f + 2v^2 f' & 0 & \frac{il}{r} & -2uvf' - \partial_r - \frac{1}{r} \\ 2uvf' - \partial_r & \frac{il}{r} & 0 & -m - \omega + f - 2u^2 f' \\ -\frac{il}{r} & -\partial_r & m + \omega - f & 0 \end{bmatrix}, \quad (2.25)$$

which does not depend on θ and ∂_θ . It follows that \mathcal{X}_l is an invariant subspace of \mathcal{A} . \square

Meanwhile, $L^2(\mathbb{R}^2, \mathbb{C}^4) = \bigoplus_{l \in \mathbb{Z}} \mathcal{X}_l$. By Lemma 2.2.1 and 2.4.1, we obtain the following lemma.

Lemma 2.4.2. *For the operator \mathcal{A} we have $\sigma_p(\mathcal{A}) = \bigcup_{l \in \mathbb{Z}} \sigma_p(\mathcal{A}|_{\mathcal{X}_l})$.*

The subspaces \mathcal{X}_l play the roles as the “even” and “odd” spaces for the 1D Soler model. We can factorize \mathcal{A} and construct the Evans function for each \mathcal{X}_l . We denote the restriction operator $\mathcal{A}|_{\mathcal{X}_l}$ by \mathcal{A}_l .

2.5 Spectral Stability Analysis

2.5.1 Some Explicit Eigenvalues

Before computing the point spectrum by using Evans functions, we are able to obtain some eigenvalues and corresponding eigenfunctions explicitly.

Lemma 2.5.1. *The operator \mathcal{A} has the following eigenvalues:*

1. $\lambda_1 = 0$ on the invariant subspace \mathcal{X}_0 with the eigenfunction

$$\Psi_1 = \begin{bmatrix} 0 \\ v \\ -u \\ 0 \end{bmatrix}; \quad (2.26)$$

2. $\lambda_2 = 2\omega i$ on the invariant subspace \mathcal{X}_{-1} with the eigenfunction

$$\Psi_2 = \begin{bmatrix} -iu \\ -u \\ v \\ -iv \end{bmatrix} e^{-i\theta}. \quad (2.27)$$

Proof. We can plug in those eigenfunctions to verify that they correspond to the indicated eigenvalues. Recall the ODE system (2.7)

$$\begin{cases} v'(r) = -(m - f(v^2 - u^2) + \omega)u(r) \\ u'(r) + \frac{1}{r}u(r) = -(m - f(v^2 - u^2) - \omega)v(r) \end{cases}.$$

Since the restriction on \mathcal{A} onto \mathcal{X}_0 is given by

$$\mathcal{A}_0 = \begin{bmatrix} 0 & m - \omega - f & -\partial_r - \frac{1}{r} & 0 \\ \omega - m + f + 2v^2 f' & 0 & 0 & -2uvf' - \partial_r - \frac{1}{r} \\ 2uvf' - \partial_r & 0 & 0 & -m - \omega + f - 2u^2 f' \\ 0 & -\partial_r & m + \omega - f & 0 \end{bmatrix}, \quad (2.28)$$

we have

$$\mathcal{A}_0 \Psi_1 = \begin{bmatrix} (m - \omega - f)v + (\partial_r + \frac{1}{r})u \\ 0 \\ 0 \\ -\partial_r v - (m - f + \omega)u \end{bmatrix} = \begin{bmatrix} 0 \\ 0 \\ 0 \\ 0 \end{bmatrix},$$

and it implies that Ψ_1 is an eigenfunction associated with $\lambda_1 = 0$. Similarly, on the subspace \mathcal{X}_{-1} the restriction operator is written as

$$\mathcal{A}_{-1} = \begin{bmatrix} 0 & m - \omega - f & -\partial_r - \frac{1}{r} & \frac{i}{r} \\ \omega - m + f + 2v^2 f' & 0 & -\frac{i}{r} & -2uvf' - \partial_r - \frac{1}{r} \\ 2uvf' - \partial_r & -\frac{i}{r} & 0 & -m - \omega + f - 2u^2 f' \\ \frac{i}{r} & -\partial_r & m + \omega - f & 0 \end{bmatrix}, \quad (2.29)$$

and it follows that

$$\begin{aligned}
(\mathcal{A}_1 - 2\omega i)\Psi_2 &= \begin{bmatrix} -2\omega u - (m - \omega - f)u - (\partial_r + \frac{1}{r})v + \frac{1}{r}v \\ -i(\omega - m + f + 2v^2 f')u + 2\omega iu - \frac{i}{r}v - i(-2uvf' - \partial_r - \frac{1}{r})v \\ -i(2uvf' - \partial_r)u + \frac{i}{r}u - 2\omega iv - i(-m - \omega + f - 2u^2 f')v \\ \frac{i}{r}u + \partial_r u + (m + \omega - f)v - 2\omega v \end{bmatrix} e^{-i\theta} \\
&= \begin{bmatrix} -(m + \omega - f)u - v' \\ i(m + \omega - f)u + iv' \\ i(u + \frac{1}{r}u) + i(m - \omega - f)v \\ (u + \frac{1}{r}u) + (m - \omega - f)v \end{bmatrix} e^{-i\theta}.
\end{aligned}$$

According to the system (2.7), we know that $(\mathcal{A}_1 - 2\omega i)\Psi_2 = 0$ and $2\omega i$ is an eigenvalue with the eigenfunction Ψ_2 . \square

2.5.2 Symmetry Properties for $\sigma_p(\mathcal{A})$

The point spectrum of \mathcal{A} has some symmetry properties, which lead to computation convenience for the Evans function technique.

Lemma 2.5.2. *If $\lambda \in \sigma_p(\mathcal{A})$, then $\bar{\lambda}$, $-\lambda$ and $-\bar{\lambda}$ are all in $\sigma_p(\mathcal{A})$.*

Proof. Suppose that $\lambda \in \sigma_p(\mathcal{A}_l)$, and consider the corresponding eigenfunction:

$$\Psi = \begin{bmatrix} F_1(r) \\ G_1(r) \\ F_2(r) \\ G_2(r) \end{bmatrix} e^{i\theta}, \tag{2.30}$$

then we have $(\mathcal{A}_l - \lambda)\Psi = 0$, namely,

$$\begin{bmatrix} -\lambda & m - \omega - f & -\partial_r - \frac{1}{r} & \frac{i}{r} \\ \omega - m + f + 2v^2 f' & -\lambda & -\frac{i}{r} & -2uvf' - \partial_r - \frac{1}{r} \\ 2uvf' - \partial_r & -\frac{i}{r} & -\lambda & -m - \omega + f - 2u^2 f' \\ \frac{i}{r} & -\partial_r & m + \omega - f & -\lambda \end{bmatrix} \begin{bmatrix} F_1(r) \\ G_1(r) \\ F_2(r) \\ G_2(r) \end{bmatrix} = 0.$$

Since the only complex terms in the matrix above are λ and $\frac{il}{r}$, the following relation:

$$\begin{bmatrix} -\bar{\lambda} & m - \omega - f & -\partial_r - \frac{1}{r} & -\frac{i}{r} \\ \omega - m + f + 2v^2 f' & -\bar{\lambda} & \frac{i}{r} & -2uvf' - \partial_r - \frac{1}{r} \\ 2uvf' - \partial_r & \frac{i}{r} & -\bar{\lambda} & -m - \omega + f - 2u^2 f' \\ -\frac{i}{r} & -\partial_r & m + \omega - f & -\bar{\lambda} \end{bmatrix} \begin{bmatrix} \bar{F}_1(r) \\ \bar{G}_1(r) \\ \bar{F}_2(r) \\ \bar{G}_2(r) \end{bmatrix} = 0$$

still holds. The matrix above is just the operator $(\mathcal{A}_{-l} - \bar{\lambda})$. It implies that $\bar{\lambda} \in \sigma_p(\mathcal{A}_{-l})$ with the eigenfunction $\bar{\Psi}$. We also have the following relation

$$\begin{bmatrix} \lambda & m - \omega - f & -\partial_r - \frac{1}{r} & -\frac{i}{r} \\ \omega - m + f + 2v^2 f' & \lambda & \frac{i}{r} & -2uvf' - \partial_r - \frac{1}{r} \\ 2uvf' - \partial_r & \frac{i}{r} & \lambda & -m - \omega + f - 2u^2 f' \\ -\frac{i}{r} & -\partial_r & m + \omega - f & \lambda \end{bmatrix} \begin{bmatrix} F_1(r) \\ -G_1(r) \\ -F_2(r) \\ G_2(r) \end{bmatrix} = 0,$$

and the matrix is the operator $(\mathcal{A}_{-l} + \lambda)$. Thus, $-\lambda \in \sigma_p(\mathcal{A}_{-l})$ with the eigenfunction

$$\Phi = \begin{bmatrix} F_1(r) \\ -G_1(r) \\ -F_2(r) \\ G_2(r) \end{bmatrix} e^{-il}.$$

It follows that $-\bar{\lambda}$ is in $\sigma_p(\mathcal{A})$. □

Remark 2.5.1. We know that $2\omega i$ is also an eigenvalue for \mathcal{A} with the eigenfunction $\bar{\Psi}_2$ according to Lemma 2.5.1 and 2.5.2.

Remark 2.5.2. Lemma 2.5.2 implies that $\sigma_p(\mathcal{A})$ is symmetric with respect the real and imaginary axes. It follows that if $\lambda \in \sigma_p(\mathcal{A})$ and $\operatorname{Re}\lambda \neq 0$, then there must exist an eigenvalue with positive real part and the corresponding solitary wave is linearly unstable. The presence of symmetry can reduce the workload of numerical computation. As we apply the Evans function technique to locate eigenvalues, we can concentrate on the first quadrant of the complex plane, together with the upper half imaginary and the right half real axes, instead of considering the whole complex plane.

2.5.3 Essential Spectrum of \mathcal{A}

It is crucial to study the essential spectrum of \mathcal{A} since the eigenvalues with non-zero real parts may arise from the threshold of $\sigma_{\text{ess}}(\mathcal{A})$ or eigenvalues embedded into $\sigma_{\text{ess}}(\mathcal{A})$.

Lemma 2.5.3. For the operator \mathcal{A} , the essential spectrum is given by

$$\sigma_{\text{ess}}(\mathcal{A}) = i\mathbb{R} \setminus (-i(m - \omega), i(m - \omega)). \quad (2.31)$$

Proof. Since $u, v, f(u^2 - v^2)$ and $f'(u^2 - v^2)$ all decay rapidly as $r \rightarrow +\infty$, we can consider the essential spectrum of the limit of \mathcal{A} as $r \rightarrow +\infty$

$$\tilde{\mathcal{A}} = \begin{bmatrix} 0 & m - \omega & -\partial_r & 0 \\ \omega - m & 0 & 0 & -\partial_r \\ -\partial_r & 0 & 0 & -m - \omega \\ 0 & -\partial_r & m + \omega & 0 \end{bmatrix}, \quad (2.32)$$

instead of \mathcal{A} , by Weyl's theorem (see [20]). We note that $\tilde{\mathcal{A}}$ only contains the term ∂_r besides m and ω , and thus use the Ansatz $\Psi(r) = Y e^{i\xi r}$ with $Y \in \mathbb{C}^4$. If $(\tilde{\mathcal{A}} - \lambda)\Psi = 0$, then we have

$$(\tilde{\mathcal{A}} - \lambda)\Psi = \begin{bmatrix} B & D \\ D & C \end{bmatrix} Y e^{i\xi r} = 0 \quad (2.33)$$

where

$$B = \begin{bmatrix} -\lambda & m - \omega \\ -m + \omega & -\lambda \end{bmatrix}, \quad C = \begin{bmatrix} -\lambda & -m - \omega \\ m + \omega & -\lambda \end{bmatrix}, \quad D = \begin{bmatrix} -i\xi & 0 \\ 0 & -i\xi \end{bmatrix}. \quad (2.34)$$

The essential spectrum is the collection of values of λ which correspond to $\xi \in \mathbb{R}$ and the determinant of the block matrix introduced in Equation (2.33) equals zero. Since matrices C and D commute, we have

$$\begin{aligned} \det \begin{bmatrix} B & D \\ D & C \end{bmatrix} &= \det(BC - D^2) \\ &= \det \left(\begin{bmatrix} \lambda^2 + m^2 - \omega^2 & 2\omega\lambda \\ -2\omega\lambda & m^2 - \omega^2 + \lambda^2 \end{bmatrix} - \begin{bmatrix} -\xi^2 & 0 \\ 0 & -\xi^2 \end{bmatrix} \right) \\ &= (m^2 - \omega^2 + \xi^2 + \lambda^2) + 4\omega^2\lambda^2 = 0. \end{aligned}$$

It follows that

$$\xi = \pm \sqrt{(\omega \pm i\lambda)^2 - m^2}. \quad (2.35)$$

Therefore, we have $\lambda \in i\mathbb{R} \setminus (-i(m - \omega), i(m - \omega))$ to make $\xi \in \mathbb{R}$. \square

Definition 2.5.1 (Threshold points). *The values of λ such that ξ in Equation (2.35) vanishes are called threshold points.*

Obviously, there are four threshold points, $\pm i(m \pm \omega)$. We note that there is a gap $(-i(m - \omega), i(m - \omega))$ between the essential spectrum of \mathcal{A} . The eigenvalues with non-zero real parts may arise from the collision of purely imaginary eigenvalues in this gap.

Remark 2.5.3. *By Lemma 2.5.1 and 2.5.3, we know that $\pm 2\omega i$ are eigenvalues embedded into the essential spectrum of \mathcal{A} for $\omega > m/3$.*

2.5.4 Construction of the Evans Function

We construct the Evans function for each subspace \mathcal{X}_l . Similarly to the 1D Soler model, the Evans functions contain the solutions to $(\mathcal{A}_l - \lambda)\Phi = 0$ with suitable initial values at $r = 0$ and the Jost solutions to the same equation, which decay as $r \rightarrow +\infty$.

Let us first solve the equation near $r = 0$. For \mathcal{X}_0 we know that

$$\mathcal{A}_0 = \begin{bmatrix} 0 & m - \omega - f & -\partial_r - \frac{1}{r} & 0 \\ \omega - m + f + 2v^2 f' & 0 & 0 & -2uvf' - \partial_r - \frac{1}{r} \\ 2uvf' - \partial_r & 0 & 0 & -m - \omega + f - 2u^2 f' \\ 0 & -\partial_r & m + \omega - f & 0 \end{bmatrix},$$

which contains the term $1/r$ on the third and fourth columns. To avoid the singularity at $r = 0$, the third and fourth elements in the initial values have to be zero and thus we have to choose the initial values are

$$b_1 = \begin{bmatrix} 1 \\ 0 \\ 0 \\ 0 \end{bmatrix} \quad \text{and} \quad b_2 = \begin{bmatrix} 0 \\ 1 \\ 0 \\ 0 \end{bmatrix},$$

Then we can obtain two solutions Φ_1 and Φ_2 with initial values $\Phi_1|_{r=0} = b_1$ and $\Phi_2|_{r=0} = b_2$.

Obviously, Φ_1 and Φ_2 are linearly independent as well.

For $l \neq 0$, recall that $\mathcal{A}_l - \lambda$ is of the form

$$\begin{bmatrix} -\lambda & m - \omega - f & -\partial_r - \frac{1}{r} & \frac{i l}{r} \\ \omega - m + f + 2v^2 f' & -\lambda & -\frac{i l}{r} & -2uvf' - \partial_r - \frac{1}{r} \\ 2uvf' - \partial_r & -\frac{i l}{r} & -\lambda & -m - \omega + f - 2u^2 f' \\ \frac{i l}{r} & -\partial_r & m + \omega - f & -\lambda \end{bmatrix}.$$

In this case, it is more complicated to choose suitable initial values since each column contains the

term il/r or $1/r$. However, if $p(r) = r^a$ where $a \in \mathbb{N}$, then $p'(r) = ap(r)/r$. Therefore, if the solution behaves near the origin like a polynomial with suitable coefficients, the terms containing singular factor $1/r$ can be eliminated. Suppose that the solution to $(\mathcal{A}_l - \lambda)\Phi = 0$ is written as Equation (2.24). We know that $F_j, G_j, j = 1, 2$ are all in \mathcal{C}^1 and the space of polynomials is embedded densely into $\mathcal{C}^1[0, 1]$. Without loss of generality, for $r < 1$ we assume that

$$\begin{aligned} F_1(r) &= c_1 r^a + o(r^a), & G_1(r) &= k_1 r^a + o(r^a), \\ F_2(r) &= c_2 r^b + o(r^b), & G_2(r) &= k_2 r^b + o(r^b), \end{aligned}$$

where $a, b \in \mathbb{Z}_+$ and $c_j, k_j, j = 1, 2$ are in \mathbb{C} satisfying

$$|c_1| + |k_1| > 0, \quad |c_2| + |k_2| > 0.$$

To find possible values of c_i and k_i , we consider the following cases.

Case 1: $a = b$. Consider the leading order of r (the leading order of r is the smallest exponential since $r \in (0, 1)$) in the third and fourth rows in \mathcal{A}_l , which is going to be r^{a-1} . Collecting the terms at r^{a-1} , we obtain

$$\begin{cases} -ac_1 + ilk_1 = 0, \\ -ilc_1 - ak_1 = 0. \end{cases} \quad (2.36)$$

Since c_1 and k_1 cannot be equal to 0 simultaneously, the system above has a nontrivial solution and thus $a^2 - l^2 = 0$. It follows that $a = |l|$ and one solution is $c_1 = |l|$ and $k_1 = -il$. For the first and second rows, collecting the terms in the leading order of r (which is again r^{a-1} since $a = b$), we have the system

$$\begin{cases} -(b+1)c_2 + ilk_2 = 0, \\ -ilc_2 - (b+1)k_2 = 0. \end{cases}$$

Similarly, the relation $(b+1)^2 - l^2 = 0$ is necessary for the existence of nontrivial solutions. Hence we have $b = |l| - 1$. It follows that $a \neq b$, which contradicts the assumption $a = b$.

Case 2: $a < b$. Consider the leading order of r in the third and fourth rows in \mathcal{A}_l . Since the leading order term is also r^{a-1} , we have the same system as Equation (2.36) for c_1 and k_1 . Thus, $a = |l|$ and one solution is $c_1 = |l|$ and $k_1 = -il$. We consider the leading order of r in the first and second rows in two different cases.

Case 2A: $b = a + 1$. In this case, the leading order term is r^a (or r^{b-1}), and we obtain the system

$$\begin{cases} -\lambda c_1 + (m - \omega - f_0)k_1 - (b + 1)c_2 - ilk_2 = 0, \\ (\omega - m + f_0 + 2v_0^2 f'_0)c_1 - \lambda k_1 + ilc_2 - (b + 1)k_2 = 0, \end{cases}$$

where

$$v_0 = v(0), \quad f_0 = f(v^2 - u^2)|_{x=0}, \quad f'_0 = f'(v^2 - u^2)|_{x=0}.$$

Substituting c_1 and k_1 by $|l|$ and il , the system has a unique solution for c_2 and k_2 , which is a combination of the two solutions in **Case 3B**.

Case 2B: $b > a + 1$. The leading order term in the first and second rows is r^a and we have the following system

$$\begin{cases} -\lambda c_1 + (m - \omega - f_0)k_1 = 0, \\ (\omega - m + f_0 + 2v(0)^2 f'_0)c_1 - \lambda k_1 = 0. \end{cases}$$

There exists a nontrivial solution only if

$$\lambda^2 - (m - \omega - f_0)(\omega - m + f_0 + 2v(0)^2 f'_0) = 0.$$

However, c_1 and k_1 also satisfy the system (2.36) and it follows that $2v_0^2 f'_0 = 0$. We know that $v(0) > 0$ and thus neither v_0 nor $f'_0 = f'(v^2(0))$ is zero. The contradiction implies that there is no nonzero solution c_i and k_i .

Case 3: $a > b$. The leading order term in the first and second rows is r^{b-1} and we obtain

$$\begin{cases} -(b + 1)c_2 - ilk_2 = 0, \\ ilc_2 - (b + 1)k_2 = 0. \end{cases} \quad (2.37)$$

If the system has nontrivial solution, then $(b + 1)^2 - l^2 = 0$. It follows that $b = |l| - 1$ and one solution is $c_2 = |l|$ and $k_2 = il$. Similarly to **Case 2**, we solve for c_1 and k_1 in two distinct cases.

Case 3A: $a = b + 1$. For the third and fourth rows, with respect to the leading order term r^b we have

$$\begin{cases} -|l|c_1 + ilk_1 - \lambda c_2 - (m + \omega - f_0)k_2 = 0, \\ -ilc_1 - |l|k_1 + (m + \omega - f_0)c_2 - \lambda k_2 = 0. \end{cases}$$

Substituting c_2 and k_2 by $|l|$ and il), respectively,

$$\begin{cases} -|l|c_1 + ilk_1 - \lambda|l| - (m + \omega - f_0)il = 0, \\ -ilc_1 - |l|k_1 + (m + \omega - f_0)|l| - \lambda il = 0. \end{cases}$$

The two equations in the system above are linearly dependent, and we can choose two linearly independent solutions as:

$$d_1 = \begin{bmatrix} -\lambda - (m + \omega - f_0)\frac{il}{|l|} \\ 0 \\ |l| \\ il \end{bmatrix} \quad \text{and} \quad d_2 = \begin{bmatrix} 0 \\ -i\lambda\frac{l}{|l|} + m + \omega - f_0 \\ |l| \\ il \end{bmatrix}. \quad (2.38)$$

Case 3B: $a > b + 1$. Collect the leading order r^b of the third and forth rows in \mathcal{X}_l and we get

$$\begin{cases} -\lambda c_2 - (m + \omega - f_0)k_2 = 0, \\ (m + \omega - f_0)c_2 - \lambda k_2 = 0. \end{cases}$$

The system has nontrivial solutions only if $\lambda^2 = -(m + \omega - f_0)^2$. But c_2 and k_2 have to coincide with the system (2.37). It follows that $(m + \omega - f_0)$ is restricted to equal 1 and λ is $\pm i$. Thus, we ignore this case.

According to all the cases above, for $l \neq 0$, we set

$$F_1(r) = C_1(r)r^a, \quad G_1(r) = K_1(r)r^a, \quad F_2(r) = C_2(r)r^b, \quad G_2(r) = K_2(r)r^b,$$

where $C_j, K_j, j = 1, 2$ are in $C_1(\mathbb{R}_+, \mathbb{C})$ and $a = b + 1 = |l|$. Since $(\mathcal{A}_l - \lambda)\Phi = 0$, we have

$$\left\{ \begin{array}{l} -\lambda C_1 r^a + (m - \omega - f)K_1 r^a - C_2' r^b - b C_2 r^{b-1} - C_2 r^{b-1} - i l K_2 r^{b-1} = 0 \\ (\omega - m + f + 2v^2 f')C_1 r^a - \lambda K_1 r^a + i l C_2 r^{b-1} - 2uv f' K_2 r^b - K_2' r^b - (b + 1)K_2 r^{b-1} = 0 \\ 2uv f' C_1 r^a - C_1' r^a - a C_1 r^{a-1} + i l K_1 r^{a-1} - \lambda C_2 r^b + (-m - \omega + f - 2u^2 f')K_2 r^b = 0 \\ -i l C_1 r^{a-1} - K_1' r^a - a K_1 r^{a-1} + (m + \omega - f)C_2 r^b - \lambda K_2 r^b = 0 \end{array} \right.$$

If we define $V(r) = [C_1(r), K_1(r), C_2(r), K_2(r)]^T$, then we have the equation

$$\partial_r V = BV \tag{2.39}$$

where $B(r, \omega, \lambda)$ is defined by

$$\left[\begin{array}{cccc} 2uv f' - \frac{a}{r} & \frac{i l}{r} & -\frac{\lambda}{r} & \frac{1}{r}(-m - \omega + f - 2u^2 f') \\ -\frac{i l}{r} & -\frac{a}{r} & \frac{1}{r}(m + \omega - f) & -\frac{\lambda}{r} \\ -\lambda r & (m - \omega - f)r & -\frac{a}{r} & -\frac{i l}{r} \\ (\omega - m + f + 2v^2 f')r & -\lambda r & \frac{i l}{r} & -2uv f' - \frac{a}{r} \end{array} \right].$$

There will be two solutions V_1 and V_2 to Equation (2.39) with the initial values $V_1(0) = d_1$ and $V_2(0) = d_2$. Then we can two linearly independent solutions $\Phi_1 = DV_1 e^{il}$ and $\Phi_2 = DV_2 e^{il}$ where

$$D = \begin{bmatrix} r^a & 0 & 0 & 0 \\ 0 & r^a & 0 & 0 \\ 0 & 0 & r^b & 0 \\ 0 & 0 & 0 & r^b \end{bmatrix}. \tag{2.40}$$

We define Jost solutions for each invariant subspace \mathcal{X}_l as solutions to $(\mathcal{A}_l - \lambda)\Psi(r, \lambda) = 0$, which have the same asymptotic behavior as solutions to $(\tilde{\mathcal{A}} - \lambda)J(r, \lambda) = 0$ as $r \rightarrow \infty$, where $\tilde{\mathcal{A}}$ is defined as Equation (2.32). If λ are not the threshold points, then the solutions are of the form $J(r, \lambda) = Y(\lambda)e^{i\xi(\lambda)r}$ and the corresponding characteristic equation is

$$\det \begin{bmatrix} B & D \\ D & C \end{bmatrix} = (m^2 - \omega^2 + \xi^2 + \lambda^2) + 4\omega^2\lambda^2 = 0, \quad (2.41)$$

where the block matrix is defined by Equation (2.33). We know that Equation (2.41) has four solutions $\xi_\lambda = \pm\sqrt{(\omega \pm i\lambda)^2 - m^2}$. By the symmetry of $\sigma_p(\mathcal{A})$ (Lemma 2.5.2) we can only consider the point spectrum in the closure of the first quadrant of the complex plane and thus we take $\lambda = a + bi$ with $a \geq 0$ and $b \geq 0$. We want to choose the solutions with positive imaginary parts such that $i\xi(\lambda)$ has negative real part and $e^{i\xi(\lambda)r}$ decays exponentially at $r \rightarrow +\infty$. Hence define

$$\xi_1 = \sqrt{(\omega + b - ia)^2 - m}, \quad \xi_2 = \sqrt{(\omega - b + ia)^2 - m} \quad (2.42)$$

and for the square root we choose the branch corresponding to positive imaginary part. For convenience, the complex plane is cut by $(i(m - \omega), +i\infty) \cup (-i(m + \omega), -i\infty)$ for ξ_1 and is cut by $(i(m + \omega), +i\infty) \cup (-i(m - \omega), -i\infty)$ for ξ_2 . The corresponding solutions to $(\tilde{\mathcal{A}} - \lambda)J(r, \lambda) = 0$ are written as

$$J_1 = \begin{bmatrix} -i\xi_1 \\ \xi_1 \\ -\lambda + i(m - \omega) \\ -i\lambda - m + \omega \end{bmatrix} e^{i\xi_1 r}, \quad J_2 = \begin{bmatrix} -i\xi_2 \\ -\xi_2 \\ -\lambda - i(m - \omega) \\ i\lambda - m + \omega \end{bmatrix} e^{i\xi_2 r}. \quad (2.43)$$

We define the Evan functions for \mathcal{X}_l by

$$E_l(\lambda) = \det[\Phi_1^l, \Phi_2^l, J_1, J_2], \quad (2.44)$$

where Φ_1^l and Φ_2^l are the solutions to $(\mathcal{A}_l - \lambda)\Phi = 0$ on \mathcal{X}_l . The Wronskian-type function does not depend on r and thus it can be evaluated at $r \gg 1$. Φ_1^l and Φ_2^l are linearly independent, and so are J_1 and J_2 . If there is a $\lambda \in \mathbb{C}$ such that $E_l(\lambda) = 0$, then at least one of Φ_1^l and Φ_2^l is linearly dependent on either J_1 or J_2 ; in other words, there is at least one solution Φ_λ which is linearly dependent with either Φ_1^l or Φ_2^l near $r = 0$ and has the same asymptotic behavior as J_1 or J_2 as $r \rightarrow +\infty$, so $\Phi_\lambda \in L^2$. Then Φ_λ is an eigenfunction of \mathcal{A}_l and λ is the corresponding eigenvalue.

Remark 2.5.4. *If λ is a threshold point, say $\lambda = i(m - \omega)$, then $\xi_1 = 0$ and $J_1 = 0$. Although $E(\lambda) = 0$, we cannot conclude that λ is an eigenvalue. The Evans function can not be defined with the aid of the factorization technique in this situation since there is a zero column in $E_l(\lambda)$. It also happens for $\lambda = i(m + \omega)$.*

2.5.5 Numerical Results

We need to find the zeros of $E_l(\lambda)$. Since $E(\lambda)$ is analytic with respect to λ on the complex plane, we can use the argument principle to locate zeros.

Lemma 2.5.4 (Argument Principle). *Let $f(z)$ be an analytic function on an open set $\Omega \subset \mathbb{C}$ and D be a simple connected domain in Ω . If f never vanishes on ∂D (the boundary of D), then*

$$\frac{1}{2\pi i} \oint_{\partial D} \frac{f'(z)}{f(z)} dz = \text{number of zeros in } D, \quad (2.45)$$

where the zeros are counted with their multiplicities.

The proof can be found in standard references, for example, [49, Theorem 5.1.4].

By the definition, $E_l(\lambda)$ can only have simple zeros or double zeros. Since the double zeros may only be on the imaginary axis and the Evans function is analytic, we can plot $E_l(\lambda)$ along with the upper half imaginary axis to locate the purely imaginary eigenvalue. To look for the eigenvalues with nonzero real parts, we can place a small circle in the complex plane, which does not intersect with the imaginary axis, and numerically compute the corresponding contour integral on the left hand side of Equation (2.45). Since the value of the integral equals the number of zeros, it should

be an integer. If the value is close to an integer greater than one, it implies that there is no root of E_l in the circle; if the value is an integer greater than one, it implies that there are several zeros in the circle. In this case, we need to shrink the circle until the value becomes close to one. Then we know that there is only one zero in this circle. If the circle is very close to the imaginary axis, the semicircle can be used instead. After we obtain a circle containing only one zero inside, we want to know the exact location of the zero point. A generalized version of the argument principle can be applied.

Lemma 2.5.5. *Suppose that g and f are both analytic on a open set $\Omega \subset \mathbb{C}$, and D is a simple connected domain in Ω . If f never vanishes on ∂D and only has simple zeros, then*

$$\frac{1}{2\pi i} \oint_{\partial D} \frac{g(z)f'(z)}{f(z)} dz = \sum_{z \in S} g(z), \quad (2.46)$$

where $S = \{z \in D : f(z) = 0\}$.

Let $g(z) = z$. If the disc D contains only one zero, then

$$\frac{1}{2\pi i} \oint_{\partial D} \frac{zE_l'(z)}{E_l(z)} dz = \text{the eigenvalue of } E_l \text{ in } D. \quad (2.47)$$

Since the unstable eigenvalue (with positive real part) can only be born from the collision of discrete purely imaginary eigenvalues and the bifurcations from the origin or the threshold points or from a purely imaginary eigenvalue between the thresholds $i(m \pm \omega)$ (see [50]), we can narrow the domain for the numerical computation from the whole complex plane to a strip near the gap $(0, i(m + \omega))$. Thanks to the symmetry property of $\sigma_p(\mathcal{A})$, we can shrink the strip further to the shaded area in Figure 2.2.

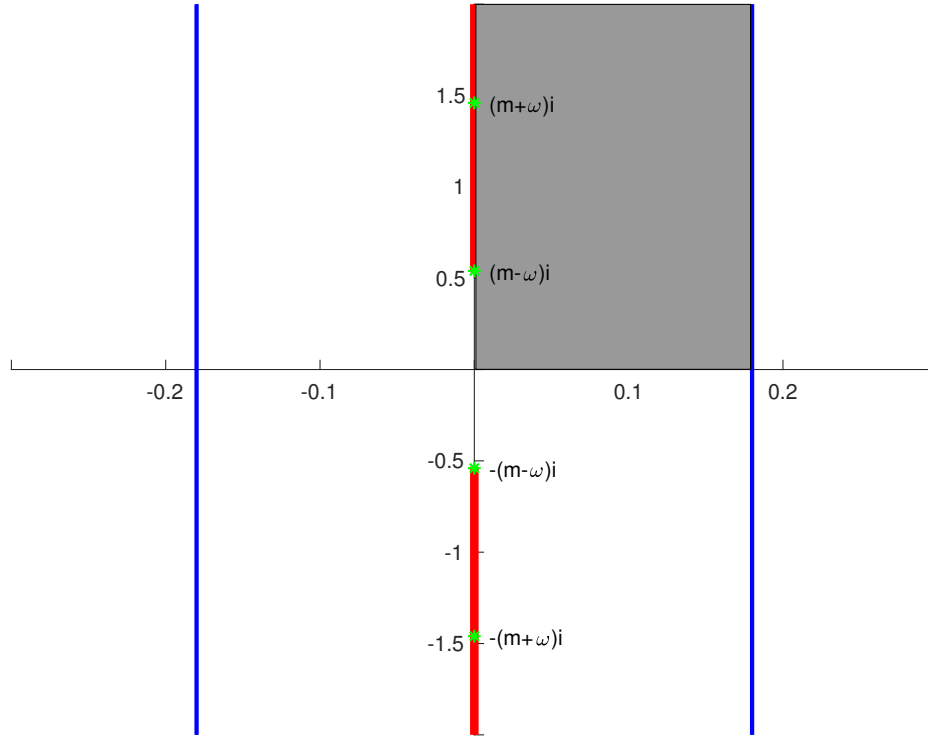


Figure 2.2: The strip between the blue lines interpret the domain to search for the eigenvalues. The red lines stand for $\sigma_{\text{ess}}(\mathcal{A})$. The green stars stand for the threshold points.

According to Figure 2.3, all the eigenvalues of \mathcal{A}_0 are purely imaginary, which implies that if the perturbation is in \mathcal{X}_0 , then the solitary wave with $\omega \in (0, 1)$ is stable. We note the zero eigenvalues in Figure 2.3, whose existence has been verified in Lemma 2.5.1. This gives a justification to the validity of our method.

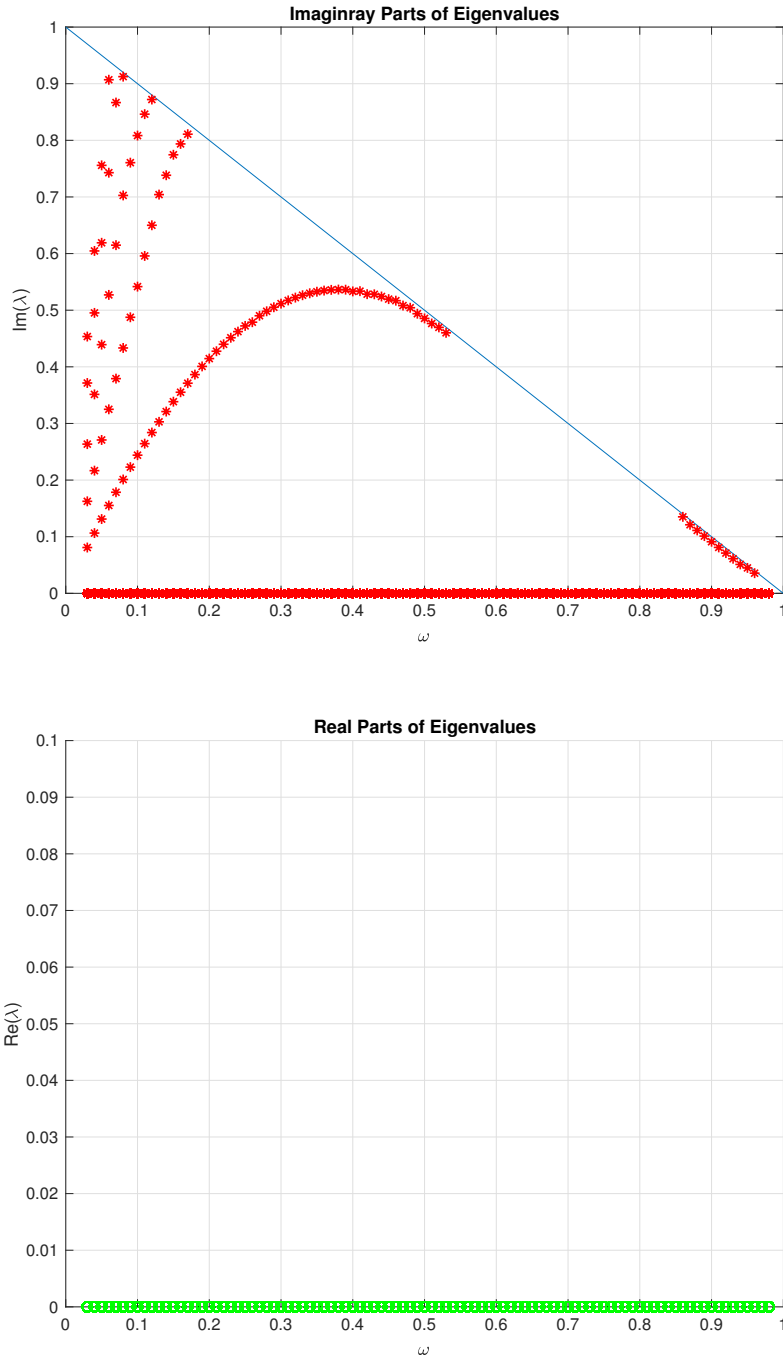


Figure 2.3: Dependence of the imaginary (red asterisks) and real (green circles) parts of the eigenvalues corresponding to \mathcal{A}_0 of ω for solitary waves in the 2D Soler model. Here we set $m = 1$ and $f(s) = s$. The triangle above the blue line corresponds to the essential spectrum of \mathcal{A}_0 .

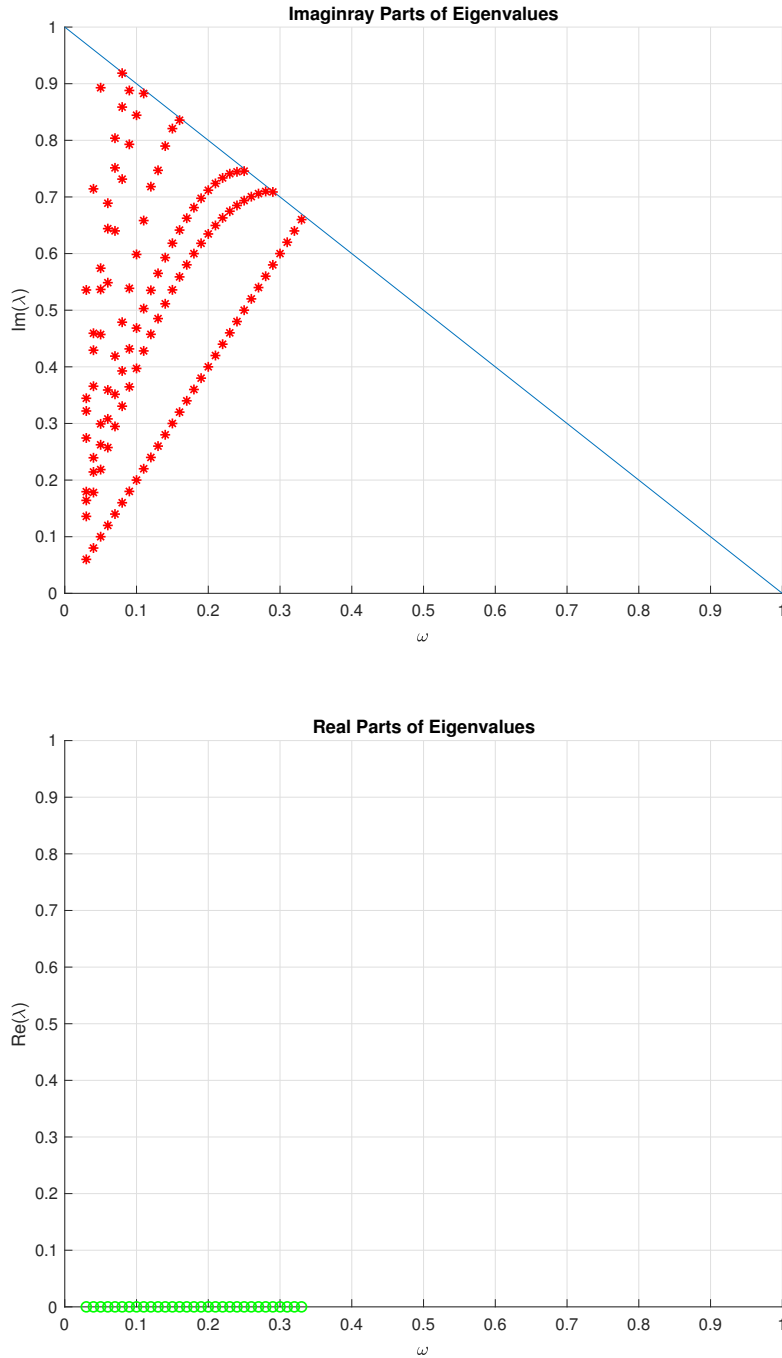


Figure 2.4: Dependence of the imaginary (red asterisks) and real (green circles) parts of the eigenvalues corresponding to $\mathcal{A}_{\pm 1}$ of ω for solitary waves in the 2D Soler model. Here we set $m = 1$ and $f(s) = s$. The triangle above the blue line corresponds to the essential spectrum of $A_{\pm 1}$. The eigenvalues embedded into the essential spectrum are ignored.

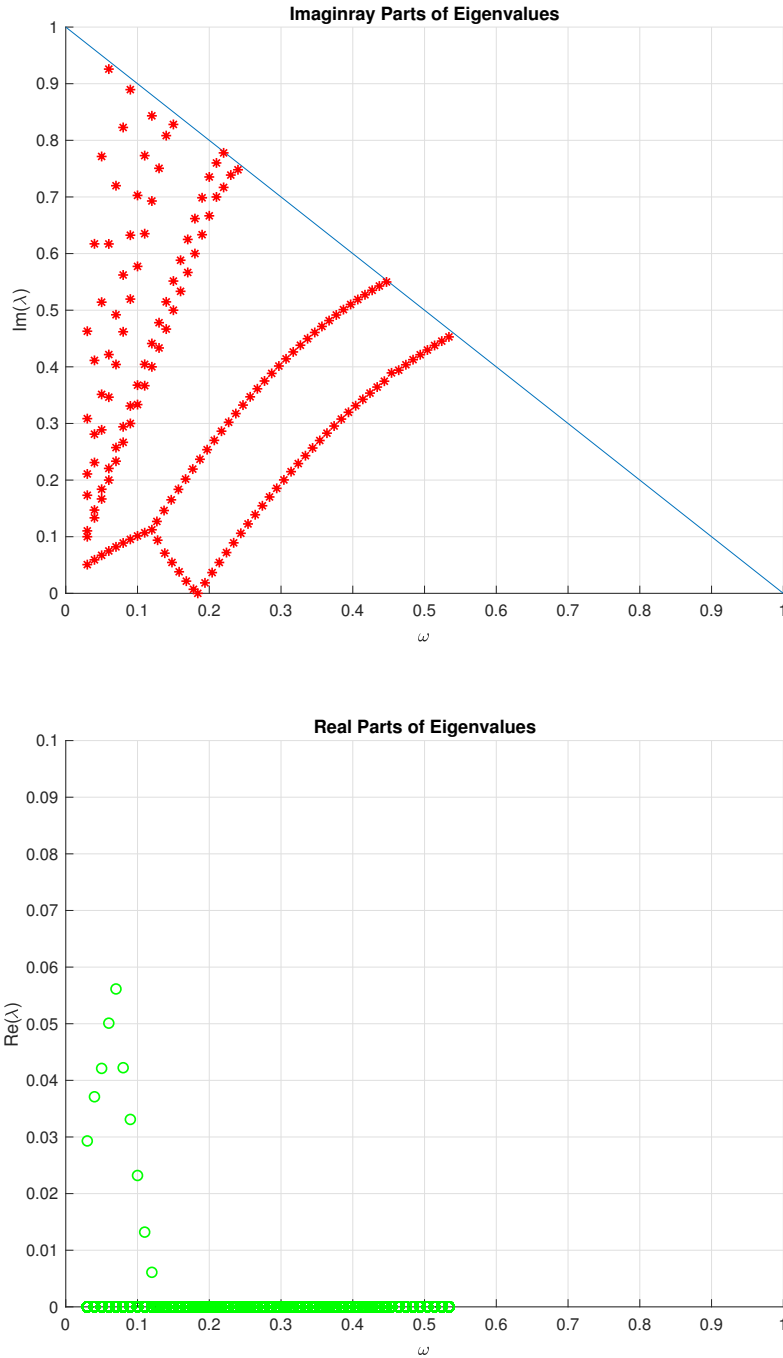


Figure 2.5: Dependence of the imaginary (red asterisks) and real (green circles) parts of the eigenvalues corresponding to $\mathcal{A}_{\pm 2}$ of ω for solitary waves in the 2D Soler model. Here we set $m = 1$ and $f(s) = s$. The triangle above the blue line corresponds to the essential spectrum of $A_{\pm 2}$.

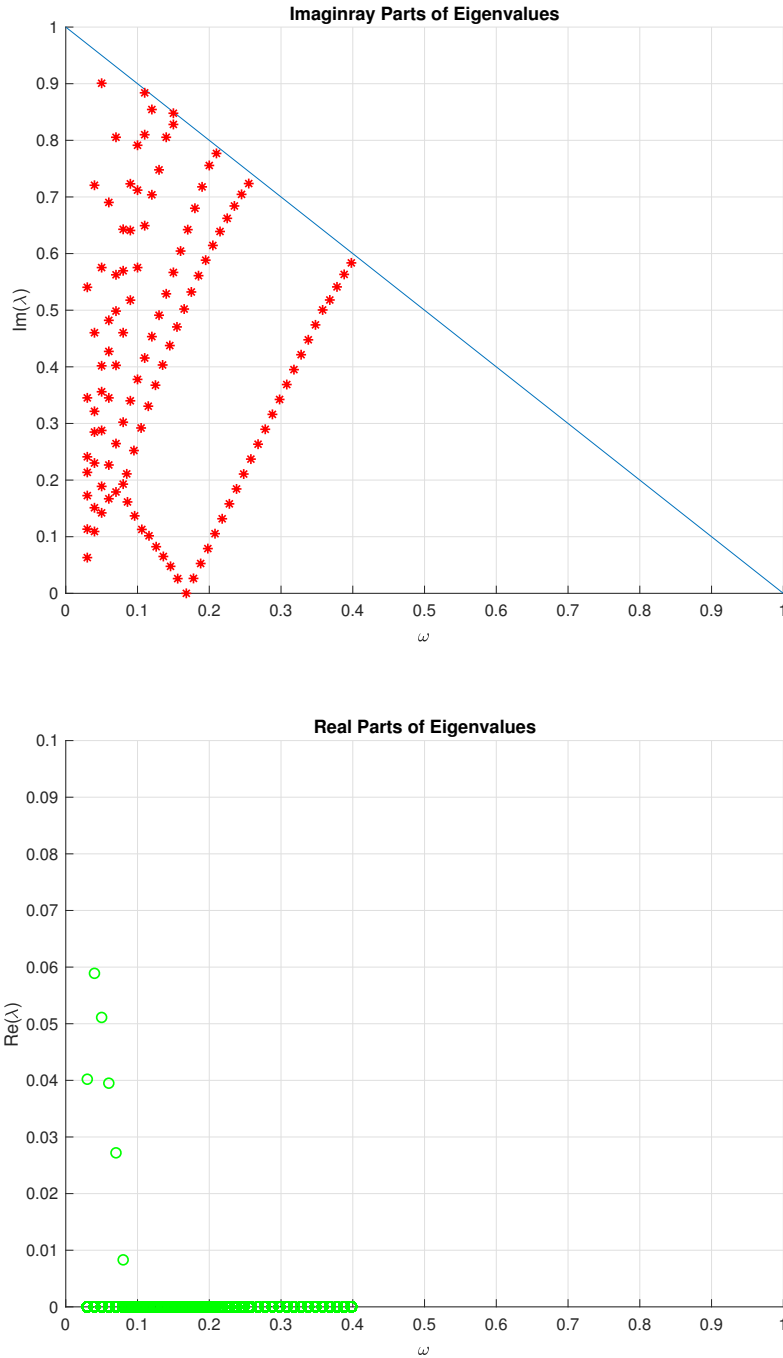


Figure 2.6: Dependence of the imaginary (red asterisks) and real (green circles) parts of the eigenvalues corresponding to $\mathcal{A}_{\pm 3}$ with respect to ω of solitary waves in the 2D Soler model. Here we set $m = 1$ and $f(s) = s$. The triangle above the blue line represents the essential spectrum of $A_{\pm 3}$.

By the symmetry property (Lemma 2.5.2), the eigenvalues of $\mathcal{A}_{\pm l}$ are plotted only in the first quadrant in the complex plane. Figure 2.4 shows that both \mathcal{A}_1 and \mathcal{A}_{-1} have no eigenvalue with positive imaginary part and thus the solitary wave is stable if the perturbation is from $\mathcal{X}_{\pm 1}$. We can observe the straight line for the eigenvalues $2\omega i$ which is shown in Lemma 2.5.1. This justifies the validity of the numerical method. In Figure 2.5 a bifurcation occurs around $\omega = 1.21$. For $\omega > 0.121$ there are no eigenvalues with positive real parts for \mathcal{A}_{-2} and \mathcal{A}_2 , but for $\omega < 0.121$ there are several eigenvalues with positive real parts. Hence the solitary wave with perturbation from $\mathcal{X}_{\pm 2}$ is no more spectrally stable when $\omega < 0.121$. In Figure 2.6 a similar bifurcation occurs around $\omega = 0.793$. For $\omega > 0.793$ there are no eigenvalues with positive real parts for \mathcal{A}_{-3} and \mathcal{A}_3 , but for $\omega < 0.793$ there are several eigenvalues with positive real parts. It follows that the solitary wave with perturbation from $\mathcal{X}_{\pm 2}$ is not spectrally stable. For larger value $|l|$, the bifurcation occurs at smaller values of ω .

2.6 Conclusion

We consider the spectral stability of the solitary wave $\phi(x)e^{-i\omega t}$ in the 2D Soler model with cubic nonlinearity. We decompose the perturbation space by the Fourier factorization and each subspace is invariant for the linearized operator \mathcal{A} . Then we apply the Evans function technique to explore $\sigma_p(\mathcal{A})$. The numerical simulation implies that the solitary waves with frequency $\omega > 0.121m$ are spectrally stable. However, the solitary waves with frequency $\omega < 0.121m$ are linearly unstable. Although the "unstable" eigenvalues have positive real parts, the magnitudes are very small and thus they are very close to the origin of the complex plane. We conclude that the unstable eigenvalues are born from the collision of the discrete purely imaginary eigenvalues between the thresholds $\pm i(m - \omega)$ when $\omega < 0.121m$.

3. 3D SOLER MODEL*

3.1 The Model

The 3D Soler model is written as

$$i\partial_t\psi = D_m\psi - f(\psi^*\beta\psi)\beta\psi, \quad \psi(x, t) \in \mathbb{C}^4, \quad x \in \mathbb{R}^3, \quad t \geq 0, \quad (3.1)$$

where $D_m = -i\alpha_1\partial_1 - i\alpha_2\partial_2 - i\alpha_3\partial_3 + \beta m$, $f(s) = s^k$, $k \in \mathbb{N}$, and Dirac matrices are defined by Equation (1.10). We can use the polar coordinates (r, θ, ϕ) defined by

$$x_1 = r \cos \phi \sin \theta, \quad x_2 = r \sin \phi \sin \theta, \quad x_3 = r \cos \theta, \quad (3.2)$$

and the corresponding Dirac operator is rewritten as

$$D_m = -i \sum_{s=r,\phi,\theta} \alpha_s \partial_s + \beta m \quad (3.3)$$

where

$$\alpha_s = \begin{bmatrix} 0 & \sigma_s \\ \sigma_s & 0 \end{bmatrix} \quad \text{for } s = r, \phi, \theta \quad (3.4)$$

and

$$\sigma_r = \begin{bmatrix} \cos \theta & e^{-i\phi} \sin \theta \\ e^{i\phi} \sin \theta & -\cos \theta \end{bmatrix}, \quad \sigma_\phi = \frac{1}{r \sin \theta} \begin{bmatrix} 0 & -ie^{-i\phi} \\ ie^{i\phi} & 0 \end{bmatrix},$$

$$\sigma_\theta = \frac{1}{r} \begin{bmatrix} -\sin \theta & e^{-i\phi} \cos \theta \\ e^{i\phi} \cos \theta & \sin \theta \end{bmatrix}.$$

*Part of this chapter is reprinted with permission from ‘‘Stability of Solitary Waves and Vortices in a 2D Nonlinear Dirac Model,’’ J. Cuevas-Maraver, P. G. Kevrekidis, A. Saxena, A. Comech, and R. Lan, 2016. *Physical Review Letters*, 116, 214101, Copyright [2016] American Physical Society.

We consider the solitary wave defined by Equation (1.22). After substituting $\psi(x, t)$ by the solitary wave we obtain an ODE system (1.23), which only depends on the radial coordinate r . For $\omega \in (0, m)$ the existence of the profile functions $u(r)$ and $v(r)$ from \mathcal{C}^1 with exponential decay at infinity have been proved. However, no explicit solutions have been presented. Similarly to 2D Soler model, we can use the shooting method to obtain the numerical solutions. Since the system is almost the same as Equation (2.7) except for the term $\frac{2}{r}u(r)$, we can mimic the procedures as in the 2D case for numerical computation. Figure 3.1 shows numerical solutions $u(r)$ and $v(r)$ for different values of ω , which are smooth enough (say in \mathcal{C}^1) and decay to zero exponentially at $r \rightarrow \infty$. Also $u(r)$ will be an odd function and $v(r)$ will be an even differentiable function if r is extended onto \mathbb{R} .

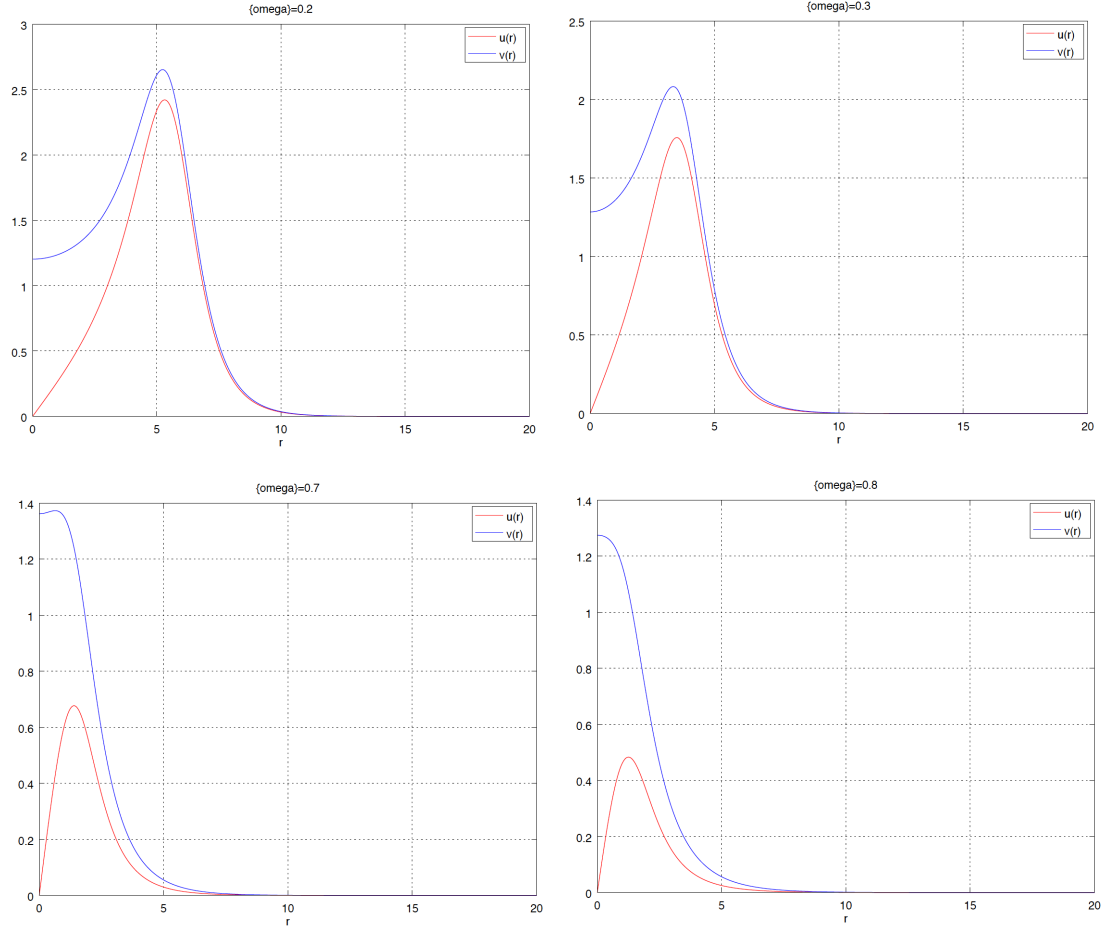


Figure 3.1: Numerical solutions u and v for different values of ω in the 3D Soler model. Here we set $m = 1$ and $f(s) = s$.

3.2 Linearization

To study the spectral stability, we need to linearize Equation (3.1). For the solitary wave

$$\psi(x, t) = \varphi(r, \theta, \phi) e^{-i\omega t} = \begin{bmatrix} v(r) \begin{bmatrix} 1 \\ 0 \end{bmatrix} \\ iu(r) \begin{bmatrix} \cos \theta \\ e^{i\phi} \sin \theta \end{bmatrix} \end{bmatrix} e^{-i\omega t},$$

we consider a perturbed solution $\psi(x, t) = (\varphi(r, \theta, \phi) + R(r, \theta, \phi, t))e^{-i\omega t}$ and linearize Equation (3.1) at the perturbation $R(r, \theta, \phi, t)$. We have

$$i\partial_t R = D_m \rho - \omega R - f\beta R - 2f' \operatorname{Re}(\varphi^* \beta R) \beta \varphi, \quad (3.5)$$

where f' and f are evaluated at $\varphi^* \beta \varphi = v^2(r) - u^2(r)$. We define

$$\mathcal{L}_3 R = D_m \rho - \omega R - f\beta R - 2f' \operatorname{Re}(\varphi^* \beta R) \beta \varphi, \quad (3.6)$$

\mathcal{L}_3 has the same property as the operator defined in Equation (2.9).

Lemma 3.2.1. *Suppose that $\varphi \in H^2(\mathbb{R}^3, \mathbb{C}^4)$ and R is an eigenfunction of \mathcal{L}_3 associated with the eigenvalue λ . Then $R \in H^2(\mathbb{R}^3, \mathbb{C}^4)$ as well.*

The lemma can be proved in the same way of Lemma 2.2.1.

We want to employ the Evans function technique to investigate the point spectrum of \mathcal{L}_3 . For the 3D case, there are two angular variables and we cannot simply use the Fourier fraction with respect to one angular variable to define the invariant space. Thus, we consider a simple case that the perturbation R has the same structure as the solitary wave profile. In consideration of the term $\operatorname{Re}(\varphi^* \beta R)$, we need to separate the real part and imaginary part of the perturbation. Therefore, we consider the perturbation in the form

$$R(r, \theta, \phi, t) = \begin{bmatrix} \begin{bmatrix} 1 \\ 0 \end{bmatrix} (R_1(r, t) + iS_1(r, t)) \\ i \begin{bmatrix} \cos \theta \\ e^{i\phi} \sin \theta \end{bmatrix} (R_2(r, t) + iS_2(r, t)) \end{bmatrix}, \quad (3.7)$$

where $R_{1,2}$ and $S_{1,2}$ are real-valued functions. Compare with 2D case, $R_{1,2}$ and $S_{1,2}$ only depend

on r and t , but not on angular variables. By substituting R by the form (3.7), we have

$$\mathcal{L}_3 R = \begin{bmatrix} \begin{pmatrix} 1 \\ 0 \end{pmatrix} F_1 \\ i \begin{pmatrix} \cos \theta \\ e^{i\phi} \sin \theta \end{pmatrix} F_2 \end{bmatrix}, \quad (3.8)$$

where

$$F_1 = R'_2 + iS'_2 + \left(\frac{2}{r} + 2f'uv\right)R_2 + \frac{2}{r}iS_2 + (m - \omega - f - 2f'v^2)R_1 + (m - \omega - f)iS_1;$$

$$F_2 = -R'_1 - iS'_1 + 2f'uvR_1 - (m + \omega - f + 2f'u^2)R_2 - (m + \omega - f)iS_2.$$

Since $i\partial_t R = \mathcal{L}_3 R$, by separating the real and imaginary parts we have

$$\partial_t \begin{bmatrix} R_1 \\ S_1 \\ R_2 \\ S_2 \end{bmatrix} = \mathcal{A} \begin{bmatrix} R_1 \\ S_1 \\ R_2 \\ S_2 \end{bmatrix}, \quad (3.9)$$

where

$$\mathcal{A} = \begin{bmatrix} 0 & m - \omega - f & 0 & \partial_r + \frac{2}{r} \\ -(m - \omega - f - 2f'v^2) & 0 & -\partial_r - \frac{2}{r} - 2f'uv & 0 \\ 0 & -\partial_r & 0 & -m - \omega + f \\ \partial_r - 2f'uv & 0 & m + \omega - f + 2f'u^2 & 0 \end{bmatrix}. \quad (3.10)$$

Remark 3.2.1. *The operator \mathcal{A} introduced above is similar to \mathcal{A}_0 in the 2D case. This similarity is due to the fact that we consider the perturbations which have the angular dependence similar to that of the solitary wave; this allows one to reduce the linearized equation to the form where the angular variables do not appear.*

3.3 Spectral Stability Analysis

3.3.1 Explicit Eigenvalue and Essential Spectrum of \mathcal{A}

Since \mathcal{A} is quite similar to \mathcal{A}_0 for the 2D Soler model, we can get some explicit eigenvalues without using the Evans functions.

Lemma 3.3.1. *The operator \mathcal{A} has an eigenvalue $\lambda = 0$ with the eigenfunction*

$$\Phi = \begin{bmatrix} 0 \\ v \\ 0 \\ u \end{bmatrix}, \quad (3.11)$$

Proof. We know that

$$\mathcal{A}\Phi = \begin{bmatrix} (m - \omega - f)v + (u' + \frac{2}{r}u) \\ 0 \\ v' + (m + \omega - f)u \\ 0 \end{bmatrix}. \quad (3.12)$$

Recall the relations in the system (1.23)

$$\begin{cases} v'(r) = -(m - f + \omega)u(r), \\ u'(r) + \frac{2}{r}u(r) = -(m - f - \omega)v(r). \end{cases}$$

It implies that $\mathcal{A}\Phi = 0$ and thus $\lambda = 0$ is an eigenvalue with the eigenfunction Φ . □

We are also interested in the essential spectrum of \mathcal{A} .

Lemma 3.3.2. *For the operator \mathcal{A} for the 3D Soler model, the essential spectrum is given by*

$$\sigma_{\text{ess}}(\mathcal{A}) = i\mathbb{R} \setminus (-i(m - \omega), i(m - \omega)). \quad (3.13)$$

Proof. By Weyl's theorem, we can consider the operator at $r \rightarrow +\infty$ instead. Due to the asymptotic behavior of u, v and f , we have

$$\tilde{\mathcal{A}} = \mathcal{A}_{r \rightarrow +\infty} = \begin{bmatrix} 0 & m - \omega & 0 & \partial_r \\ -m + \omega & 0 & -\partial_r & 0 \\ 0 & -\partial_r & 0 & -m - \omega \\ \partial_r & 0 & m + \omega & 0 \end{bmatrix}, \quad (3.14)$$

which is similar to $\tilde{\mathcal{A}}$ in 2D case and can be written as a block matrix. We just repeat the computation in the 2D case to obtain the essential spectrum. \square

Remark 3.3.1. *The essential spectrum for 1D, 2D and 3D Soler model are the same. For the 3D case, the threshold points are $\pm i(m \pm \omega)$, which are the same as in 2D case.*

3.3.2 Construction of the Evans Function

To reduce the workload of numerical computation, we investigate the symmetry properties of the point spectrum of \mathcal{A} .

Lemma 3.3.3. *If λ is an eigenvalue of \mathcal{A} , then both $\bar{\lambda}$ and $-\lambda$ are eigenvalues of \mathcal{A} .*

Proof. Suppose Φ is an eigenfunction corresponding to λ , namely, $(\mathcal{A} - \lambda)\Phi = 0$. Since \mathcal{A} is real, $\overline{\mathcal{A} - \lambda} = \mathcal{A} - \bar{\lambda}$ where $\bar{\mathcal{A}}$ is the matrix by taking the complex conjugate for each element. It follows that $(\mathcal{A} - \bar{\lambda})\bar{\Phi} = 0$ and thus $\bar{\lambda}$ is also an eigenvalue with the eigenfunction $\bar{\Phi}$. Suppose that $\Phi = [F_1, F_2, F_3, F_4]^T$. Then we have:

$$(\mathcal{A} - \lambda)\Phi = (\mathcal{A} + \lambda) \begin{bmatrix} F_1 \\ -F_2 \\ F_3 \\ -F_4 \end{bmatrix}, \quad (3.15)$$

which implies that $-\lambda$ is also an eigenvalue of \mathcal{A} associated with the eigenfunction $[F_1, -F_2, F_3, -F_4]^T$.

\square

This lemma shows that $\sigma_p(\mathcal{A})$ is symmetric with respect to the real and imaginary axes, respectively. Therefore it suffices to consider the closure of the first quadrant of the complex plane.

We know that

$$\mathcal{A} - \lambda = \begin{bmatrix} -\lambda & m - \omega - f & 0 & \partial_r + \frac{2}{r} \\ -(m - \omega - f - 2f'v^2) & -\lambda & -\partial_r - \frac{2}{r} - 2f'uv & 0 \\ 0 & -\partial_r & -\lambda & -m - \omega + f \\ \partial_r - 2f'uv & 0 & m + \omega - f + 2f'u^2 & -\lambda \end{bmatrix}, \quad (3.16)$$

and the term $\frac{2}{r}$ appears in the third and fourth columns. Hence we can choose the vectors

$$\begin{bmatrix} 1 \\ 0 \\ 0 \\ 0 \end{bmatrix} \quad \text{and} \quad \begin{bmatrix} 0 \\ 1 \\ 0 \\ 0 \end{bmatrix}$$

as the initial values for the equation $(\mathcal{A} - \lambda)\Phi = 0$ and the corresponding solutions are denoted by Φ_1 and Φ_2 , respectively.

To construct the Jost solutions, we consider the solutions to $(\mathcal{A} - \lambda)\Phi(r, \lambda) = 0$ with the same asymptotic behavior as the solutions to $(\tilde{\mathcal{A}} - \lambda)J(r, \lambda) = 0$ at $r \rightarrow +\infty$. Similarly, if λ is not a threshold point, we assume that the solution is of the form $J(r, \lambda) = Y(\lambda)e^{i\xi(\lambda)r}$. Then we obtain the characteristic equation which is the same as Equation (2.41). Let $\lambda = a + bi$ with $a \geq 0$ and $b \geq 0$ due to the symmetry property of $\sigma_p(\mathcal{A})$. We define ξ as in Equation (2.42) and choose the branch with positive imaginary parts (the complex plane is cut in the same way as in 2D case). Recall that

$$\xi_1 = \sqrt{(\omega + b - ia)^2 - m}, \quad \xi_2 = \sqrt{(\omega - b + ia)^2 - m}.$$

Then the solutions to $(\tilde{\mathcal{A}} - \lambda)J(r, \lambda)$ are written as

$$J_1 = \begin{bmatrix} -i\xi_1 \\ \xi_1 \\ -i\lambda - m + \omega \\ \lambda - i(m - \omega) \end{bmatrix} e^{i\xi_1 r} \quad \text{and} \quad J_2 = \begin{bmatrix} -i\xi_2 \\ -\xi_2 \\ i\lambda - m + \omega \\ \lambda + i(m - \omega) \end{bmatrix} e^{i\xi_2 r}. \quad (3.17)$$

Now we can define the Evans function for \mathcal{A} by

$$E(\lambda) = \det[\Phi_1, \Phi_2, J_1, J_2], \quad (3.18)$$

which will only depend on λ . The value of λ will be an eigenvalue of \mathcal{A} if $E(\lambda)$ equals zero.

3.3.3 Numerical Results

We apply the same numerical scheme as the 2D Soler model to plot the eigenvalues of \mathcal{A} in the 3D model. Since we only consider the perturbation in the same structure as the solitary wave profile, it is analogous to the plot for \mathcal{A}_0 in 2D Soler model.

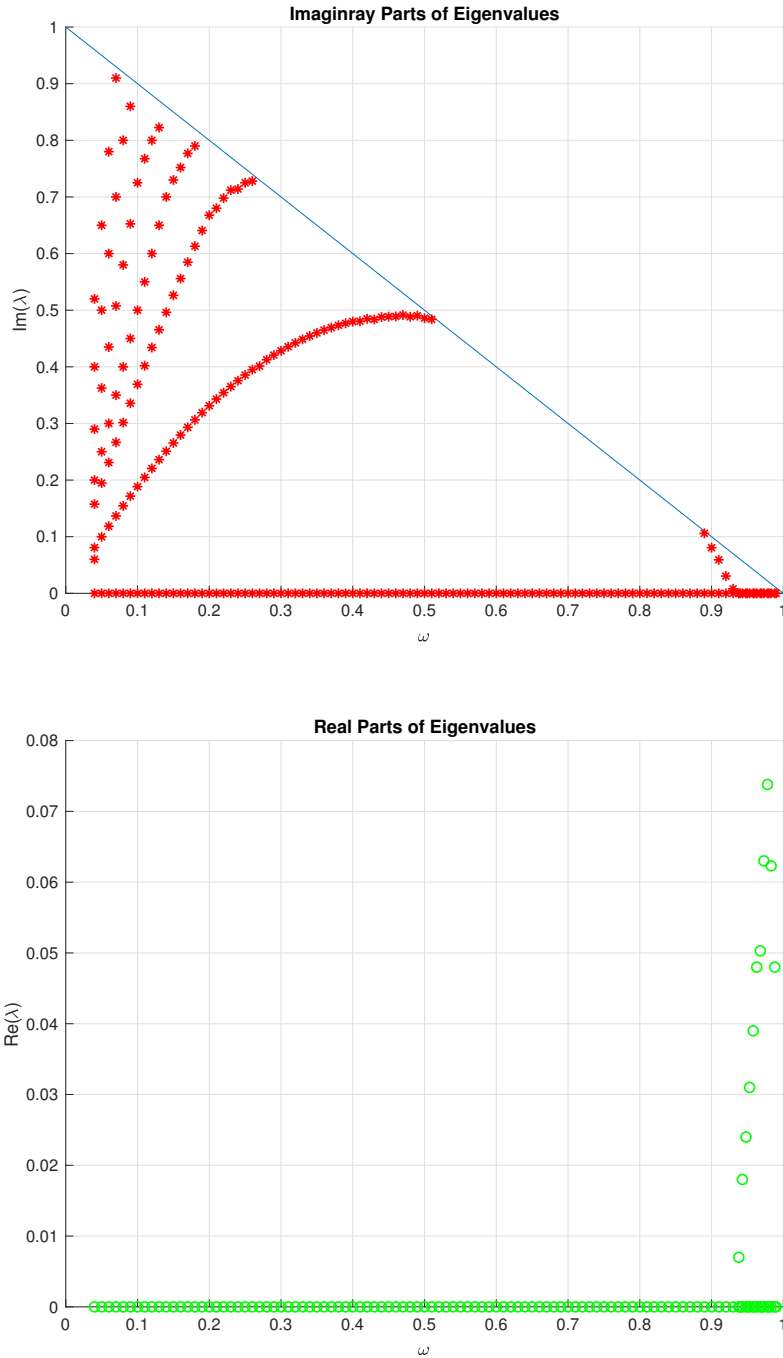


Figure 3.2: Dependence of the imaginary (red asterisks) and real (green circles) parts of the eigenvalues corresponding to \mathcal{A} with respect to ω of solitary waves in the 3D Soler model. Here we set $m = 1$ and $f(s) = s$. The triangle above the blue line represents the essential spectrum of A .

Contrary to 1D case and the invariant subspace \mathcal{X}_0 in 2D case (Figure 2.3), there are eigenvalues with positive real parts for $\omega > 0.936$. Hence the solitary waves corresponding to these values of ω are linearly unstable.

3.4 Conclusion

We study the spectral stability for the 3D Soler model with cubic nonlinearity at a solitary wave $\phi(x)e^{-i\omega t}$. We choose the perturbations which have the angular dependence similar to that of the solitary wave, and employ the Evans function technique to locate the eigenvalues of the linearized operator \mathcal{A} . The numerical simulation demonstrates that there is an eigenvalue with positive real part for $\omega > 0.936m$ and thus the corresponding solitary waves are linearly unstable. This result is in agreement with the linear instability of weakly relativistic solitary waves with $\omega \lesssim m$ in the 3D Soler model with cubic nonlinearity proved in [51]. We note that for $\omega \in (0.936m, m)$ the unstable eigenvalue (with positive real part) is purely real and when $\omega = 0.936m$ this unstable eigenvalue collides with its opposite at $\lambda = 0$. For $\omega < 0.936m$ (after the collision), this pair of eigenvalues move to the imaginary axis.

The collision of eigenvalues at $\omega = 0.936$ follows from the Vakhitov–Kolokolov condition $dQ(\omega)/d\omega = 0$ from [22, 52] which also plays the role for the nonlinear Dirac equation [53]: indeed, by [11], the charge of the solitary waves in 3D cubic Soler model has a minimum at $\omega \approx 0.936m$. What has not been known, it is whether the positive eigenvalue disappears for $\omega \lesssim 0.936m$ or whether the second positive eigenvalue is born; see [53]. Our numerical work completely resolved this question, showing that when $\omega \approx 0.936m$, the positive eigenvalue collides with its opposite, and for $\omega \lesssim 0.936m$ two purely imaginary eigenvalues are born, hence the spectral stability is expected.

3.4.1 Future work

Since we only consider a special case of the perturbation, we have no definite results for the frequency $\omega < 0.936m$. For the restriction operator \mathcal{A}_l with $l > 2$, there are eigenvalues with positive real parts when ω is small. We expect the similar results on the 3D Soler model. In the

future, the invariant spaces for general perturbations should be addressed. The spherical harmonic may play an important role for defining the invariant subspaces.

4. COULOMB-TYPE MODEL

4.1 The Model

We consider the nonlinear Dirac equation

$$i\partial_t\psi = D_m\psi - V\psi, \quad \psi(x, t) \in \mathbb{C}^2, \quad x \in \mathbb{R}, \quad t \geq 0 \quad (4.1)$$

where $D_m = -i\alpha\partial_x + \beta m$ is same as Equation (1.12), namely,

$$\alpha = -\sigma_2 = \begin{bmatrix} 0 & i \\ -i & 0 \end{bmatrix}, \quad \beta = \sigma_3 = \begin{bmatrix} 1 & 0 \\ 0 & -1 \end{bmatrix}, \quad (4.2)$$

and V is defined by $V = |\psi|^2$. We assume that Equation (4.1) has a solitary wave solution $\psi = \varphi_\omega(x)e^{-i\omega t}$, $\omega \in (0, m)$, with the profile function

$$\varphi_\omega(x) = \begin{bmatrix} v(x) \\ u(x) \end{bmatrix}. \quad (4.3)$$

Here u and v are both real-valued and from $H^1(\mathbb{R})$. Moreover, u will be an odd function and v will be an even function. After substituting ψ by the solitary wave, we can obtain an ODE system

$$\begin{cases} \omega v = u' + mv - (u^2 + v^2)v, \\ \omega u = -v' - mu - (u^2 + v^2)u, \end{cases} \quad (4.4)$$

which only depends on the spatial variable x , not the time variable t . We intend to explore the spectral stability of the solitary waves at the nonrelativistic limit $\omega \lesssim m$. We need to show the existence of the solitary wave solutions first.

4.2 The Existence of the Solitary Wave Solutions

Lemma 4.2.1. *For $0 < \omega < m$, the system (4.4) has solutions $u(x), v(x) \in H^1(\mathbb{R})$. Moreover, $u(x)$ and $v(x)$ are odd and even, respectively, and both have exponential decay at infinity.*

We will use Theorem 5 in [24] to prove the lemma. The following is the statement of the theorem.

Theorem 4.2.1 (Theorem 5 in [24]). *Let $f \in C(\mathbb{R}, \mathbb{R})$ be a locally Lipschitz continuous function with $f(0) = 0$. Let $F(z) = \int_0^z f(s) dx$. The necessary and sufficient condition for the existence of a solution u of the problem*

$$-u'' = f(u), \quad u \in C^2(\mathbb{R}), \quad \lim_{x \rightarrow \pm\infty} u = 0, \quad (4.5)$$

and $u(x_0) > 0$ for some $x_0 \in \mathbb{R}$ is that $\zeta_0 = \inf\{\zeta > 0; F(\zeta) = 0\}$ exists and $f(\zeta_0) > 0$. Furthermore, there is a unique solution up to translations of the origin, and this solution satisfies (after a suitable translation of the origin):

- i. $u(x) = u(-x), x \in \mathbb{R}$ ("u is radial"),*
- ii. $u(x) > 0, x \in \mathbb{R}$,*
- iii. $u(0) = \zeta_0$,*
- iv. $u'(x) < 0, x > 0$.*
- v. If there exists $\delta > 0$ such that $\lim_{s \rightarrow 0} \frac{f(s)}{s} \leq -\delta$ then u, u' and u'' have exponential decay at infinity.*

Before a rigorous proof, let us show the lemma instinctively and roughly. We assume that $|v| \gg |u|$ and neglect the term $(u^2 + v^2)u$ in the second equation of the system (4.4). We obtain that $v' = -(\omega + m)u$ and thus

$$-v'' = -(m^2 - \omega^2)v + (m + \omega)v^3. \quad (4.6)$$

By Theorem 4.2.1, we can show that Equation (4.6) has a unique solution with the initial value $v(0) = \sqrt{2(m - \omega)}$.

By applying the shooting method, we obtain the numerical solutions for the profile functions u and v , which are plotted in Figure 4.1. Now we present the proof of Lemma 4.2.1.

Proof. We show the existence by analyzing the Hamiltonian system corresponding to (4.4), with x playing the role of time,

$$\begin{cases} u' = \omega v - mv + (u^2 + v^2)v = \partial_v h(v, u), \\ -v' = \omega u + mu + (u^2 + v^2)u = \partial_u h(v, u), \end{cases} \quad (4.7)$$

where

$$h(v, u) = \frac{1}{2}\omega(v^2 + u^2) + \frac{1}{4}(v^2 + u^2)^2 - \frac{1}{2}m(v^2 - u^2). \quad (4.8)$$

The pair (v, u) in the solitary wave corresponds the trajectory of the Hamiltonian system such that

$$\lim_{x \rightarrow \pm\infty} v(x) = \lim_{x \rightarrow \pm\infty} u(x) = 0.$$

and hence $\lim_{x \rightarrow \pm\infty} h(v, u) = 0$. Since $h(v, u)$ is implicitly x -dependent, $h(v, u)$ is a constant and thus $h(v, u) \equiv 0$. It implies that

$$v^2 - u^2 = \frac{\omega}{m}(v^2 + u^2) + \frac{1}{2m}(v^2 + u^2)^2. \quad (4.9)$$

We introduce auxiliary functions

$$X(x) = u^2(x) + v^2(x), \quad Y(x) = u(x)v(x). \quad (4.10)$$

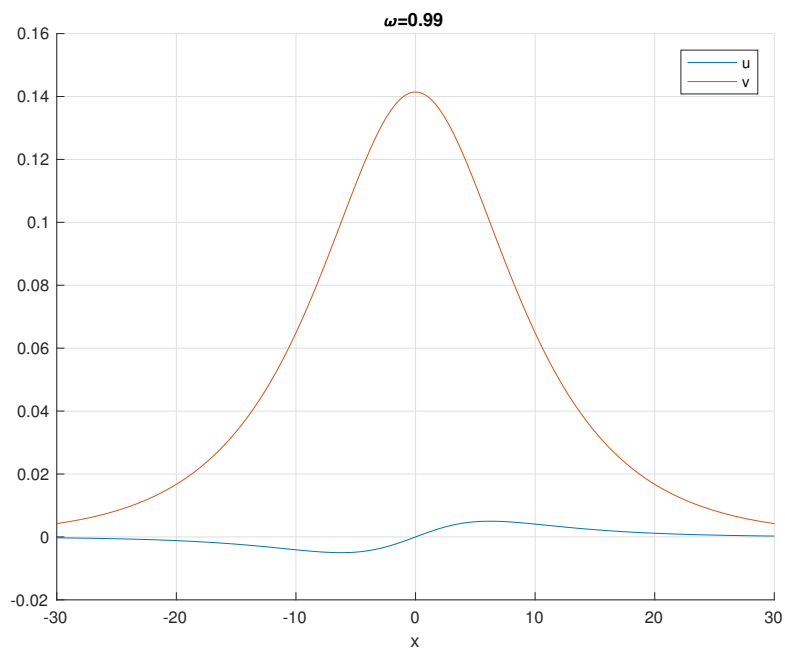
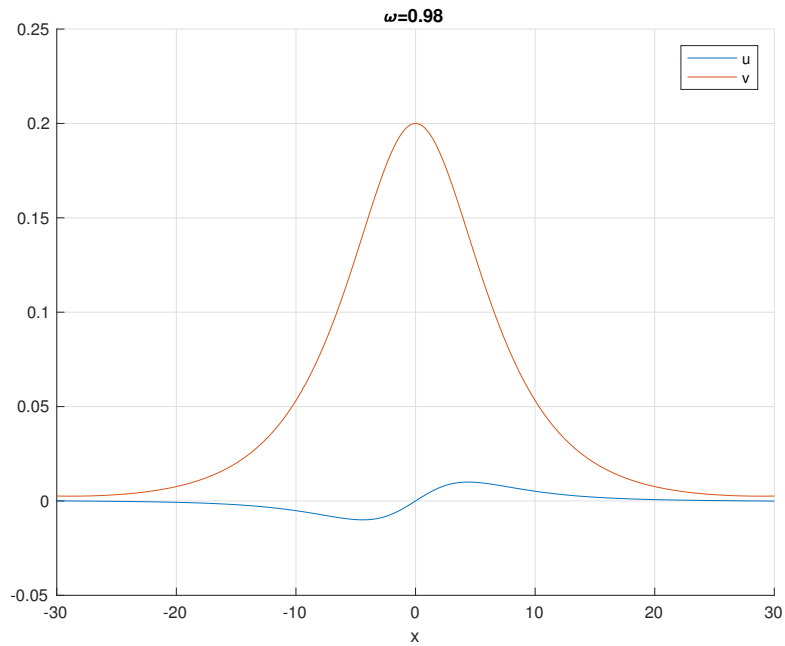


Figure 4.1: Numerical solutions u and v to the system (4.4) for the frequency ω close to $m = 1$.

By Equations (4.7), (4.9) and (4.10) we have that

$$\begin{aligned}
X'(x) &= 2uu' + 2vv' \\
&= 2u(\omega v - mv + (u^2 + v^2)v) - 2v(\omega u + mu + (u^2 + v^2)u) \\
&= -4muv,
\end{aligned}$$

and

$$\begin{aligned}
Y'(x) &= u'v + uv' \\
&= v(\omega v - mv + (u^2 + v^2)v) - u(\omega u + mu + (u^2 + v^2)u) \\
&= \omega(v^2 - u^2) - m(v^2 + u^2) + (u^2 + v^2)(v^2 - u^2) \\
&= \frac{\omega^2}{m}(v^2 + u^2) + \frac{\omega}{2m}(v^2 + u^2)^2 - m(v^2 + u^2) + \frac{\omega}{m}(v^2 + u^2)^2 + \frac{1}{2m}(v^2 + u^2)^3 \\
&= \left(\frac{\omega^2}{m} - m\right)(u^2 + v^2) + \frac{3\omega}{2m}(u^2 + v^2)^2 + \frac{1}{2m}(u^2 + v^2)^3.
\end{aligned}$$

Consequently, we obtain the system

$$\begin{cases} X' = -4mY, \\ Y' = \left(\frac{\omega^2}{m} - m\right)X + \frac{3\omega}{2m}X^2 + \frac{1}{2m}X^3, \end{cases} \quad (4.11)$$

and it can be rewritten as a second order equation with respect to X :

$$-X'' = 4(\omega^2 - m^2)X + 6\omega X^2 + 2X^3. \quad (4.12)$$

Let $f(X) = 4(\omega^2 - m^2)X + 6\omega X^2 + 2X^3$. Then we have $f(0) = 0$ and

$$F(z) = \int_0^z f(X)dX = \frac{1}{2}z^4 + 2\omega z^3 + 2(\omega^2 - m^2)z^2. \quad (4.13)$$

It follows that $\zeta_0 = \inf\{\zeta > 0; F(\zeta) = 0\} = 2(m - \omega)$ and

$$f(\zeta_0) = 4(\omega^2 - m^2)\zeta_0 + 6\omega\zeta_0^2 + 2\zeta_0^3 = 8m(\omega - m)(\omega - 2m + 1).$$

If we take $m = 1$, then $f(\zeta_0) > 0$ for all $\omega \in (0, m)$. By Theorem 4.2.1, we know that there is a unique solution $X \in \mathcal{C}^2$ which is positive and even, and $X'(r)$ is negative for $r > 0$. Since $X' = 4mY$, we know that $Y \in \mathcal{C}^1$ is odd and $Y(r) > 0$ for $r > 0$. Moreover, we have the initial values $X(0) = 2(m - \omega)$ and $Y(0) = 0$. Since

$$\lim_{s \rightarrow 0} \frac{f(s)}{s} = 4(\omega^2 - m^2) < 0, \quad (4.14)$$

X and Y both have exponential decay at infinity. By relations in Equation (4.10) and the restriction that u is odd and v is even, we can obtain $u, v \in \mathcal{C}^1$ uniquely with the initial values $u(0) = 0$ and $v(0) = \sqrt{2(m - \omega)}$. Since u and v also exponentially decay at infinity, u and v are in H^1 . \square

Remark 4.2.1. *The initial value $v(0) = \sqrt{2(m - \omega)}$ coincides with the “rough proof”.*

4.3 Linearization

We consider the solitary wave solutions with a perturbation ρ in the form of $\psi = (\varphi(x) + \rho(x, t))e^{-i\omega t}$ and linearize Equation (4.1) on ρ . The linearized equation is written as

$$i\partial_t \rho = D_m \rho - \omega \rho - |\varphi|^2 \rho - 2\text{Re}(\varphi^* \rho) \varphi \quad (4.15)$$

and we define the operator by

$$\mathcal{L} = D_m - \omega - |\varphi|^2 - 2\text{Re}(\varphi^* \cdot) \varphi. \quad (4.16)$$

Due to the last term in (4.15), \mathcal{L} is \mathbb{R} -linear, but not \mathbb{C} -linear. To obtain a \mathbb{C} -linear operator, we separate the real and imaginary parts of φ and ρ , and write them as

$$\varphi = \begin{bmatrix} \operatorname{Re} \varphi \\ \operatorname{Im} \varphi \end{bmatrix} \in \mathbb{R}^4, \quad \rho = \begin{bmatrix} \operatorname{Re} \rho \\ \operatorname{Im} \rho \end{bmatrix} \in \mathbb{R}^4.$$

We also rewrite the related matrices as the following:

$$\alpha = \begin{bmatrix} \operatorname{Re} \alpha & -\operatorname{Im} \alpha \\ \operatorname{Im} \alpha & \operatorname{Re} \alpha \end{bmatrix}, \quad \beta = \begin{bmatrix} \operatorname{Re} \beta & -\operatorname{Im} \beta \\ \operatorname{Im} \beta & \operatorname{Re} \beta \end{bmatrix}, \quad \mathbf{J} = \begin{bmatrix} 0 & I_2 \\ -I_2 & 0 \end{bmatrix}, \quad (4.17)$$

where α and β are defined in Equation (4.2), and I_k is the $k \times k$ identity matrix. We note that

$$\mathbf{J}^2 = -I_4, \quad \mathbf{J}\alpha = \alpha\mathbf{J}, \quad \mathbf{J}\beta = \beta\mathbf{J}. \quad (4.18)$$

Remark 4.3.1. *In the matrix form, \mathbf{J} plays the role as $-\mathrm{i}$ in the original equation.*

The term containing φ in Equation (4.16) can be rewritten as

$$\mathbf{V}\rho = -\varphi^* \varphi \rho - 2(\varphi^* \rho) \varphi,$$

and \mathbf{V} is Hermitian in the explicit form:

$$\mathbf{V} = \begin{bmatrix} -u^2 - 3v^2 & -2uv & 0 & 0 \\ -2uv & -3u^2 - v^2 & 0 & 0 \\ 0 & 0 & -u^2 - v^2 & 0 \\ 0 & 0 & 0 & -u^2 - v^2 \end{bmatrix}. \quad (4.19)$$

Then the \mathbb{C} -linear operator corresponding to (4.16) is

$$\mathbf{L} = \mathbf{J}\alpha\partial_x + m\beta - \omega + \mathbf{V} \quad (4.20)$$

and (4.15) is written as

$$-J\partial_t\rho = L\rho \quad \text{or} \quad \partial_t\rho = JL\rho. \quad (4.21)$$

4.4 Spectral Stability Analysis

4.4.1 Essential Spectrum and Symmetry Properties

By Weyl's theorem, JL has the same essential spectrum as the linearized operator in 1D Soler model and thus $\sigma_{\text{ess}}(JL) = i\mathbb{R} \setminus (-i(m - \omega), i(m - \omega))$. The threshold points for JL are $\pm i(m \pm \omega)$. The operator JL has the following symmetry properties.

Lemma 4.4.1. *The point spectrum $\sigma_p(JL)$ is symmetric with respect to the real and imaginary axes.*

Proof. We note that JL are real-valued. Suppose that $\lambda \in \sigma_p(JL)$ with the eigenfunction ψ . Then $\overline{JL\psi} = \overline{\lambda\psi} = \bar{\lambda}\bar{\psi}$. However, $\overline{JL\psi} = JL\bar{\psi}$. It follows that $\bar{\lambda}$ is also an eigenvalue of JL and $\sigma_p(JL)$ is symmetric with respect to the real axis. Define

$$K = \begin{pmatrix} I_2 & 0 \\ 0 & -I_2 \end{pmatrix}.$$

It is simple to check that $LK = KL$ and $JK = -KJ$. We have

$$JLK\psi = JKL\psi = -KJL\psi = K\lambda\psi = -\lambda K\psi$$

and thus $-\lambda$ is an eigenvalue of JL . So $\sigma_p(JL)$ is symmetric with respect to the origin in \mathcal{C} . It follows that $\sigma_p(JL)$ is also symmetric with respect to the imaginary axis. \square

4.4.2 Eigenvalues near $2\omega i$ in the Nonrelativistic Limit

Since the toy Coulomb model is not $SU(1, 1)$ symmetric, it may no longer have the eigenvalue $2\omega i$. We want to investigate if there exists an eigenvalue corresponding to $2\omega i$ of the Soler model, especially in the nonrelativistic limit, namely, $\omega \lesssim m$.

We compare the linearized operator of the toy Coulomb model to that of the Soler model. To avoid ambiguity, the linearized operators for the Soler and the toy Coulomb models are denoted by

$$\mathbf{L}_s = \mathbf{J}\boldsymbol{\alpha}\partial_x + m\boldsymbol{\beta} - \omega + \mathbf{V}_s, \quad (4.22)$$

$$\mathbf{L}_c = \mathbf{J}\boldsymbol{\alpha}\partial_x + m\boldsymbol{\beta} - \omega + \mathbf{V}_c, \quad (4.23)$$

respectively, with the Hermitian matrices

$$\mathbf{V}_s = \begin{bmatrix} -u_s^2 - 3v_s^2 & 2u_s v_s & 0 & 0 \\ 2u_s v_s & v_s^2 - 3u_s^2 & 0 & 0 \\ 0 & 0 & -v_s^2 + u_s^2 & 0 \\ 0 & 0 & 0 & v_s^2 - u_s^2 \end{bmatrix} \quad (4.24)$$

and

$$\mathbf{V}_c = \begin{bmatrix} -u_c^2 - 3v_c^2 & -2u_c v_c & 0 & 0 \\ -2u_c v_c & -3u_c^2 - v_c^2 & 0 & 0 \\ 0 & 0 & -u_c^2 - v_c^2 & 0 \\ 0 & 0 & 0 & -u_c^2 - v_c^2 \end{bmatrix}, \quad (4.25)$$

where v_s and u_s stand for the profile functions of the solitary wave solutions of the Soler model, and v_c and u_c correspond to toy Coulomb model. Both v_s and v_c have the same initial values, more precisely, $v_s(0) = v_c(0) = \sqrt{2(m - \omega)}$. Numerically, it turns out that $v_c(x) \geq v_s(x)$ for any $x \in \mathbb{R}$ (see Figure 4.2). According to matrices (4.24) and (4.25), the difference between \mathbf{L}_s and \mathbf{L}_c is

$$\begin{bmatrix} 3(v_c^2 - v_s^2) + (u_s^2 + u_c^2) & 2(u_c v_c + u_s v_s) & 0 & 0 \\ 2(v_c u_c + v_s u_s) & (v_s^2 + v_c^2) + 3(u_c^2 - u_s^2) & 0 & 0 \\ 0 & 0 & (v_c^2 - v_s^2) + (u_s^2 + u_c^2) & 0 \\ 0 & 0 & 0 & (v_c^2 + v_s^2) + (u_c^2 - u_s^2) \end{bmatrix}.$$

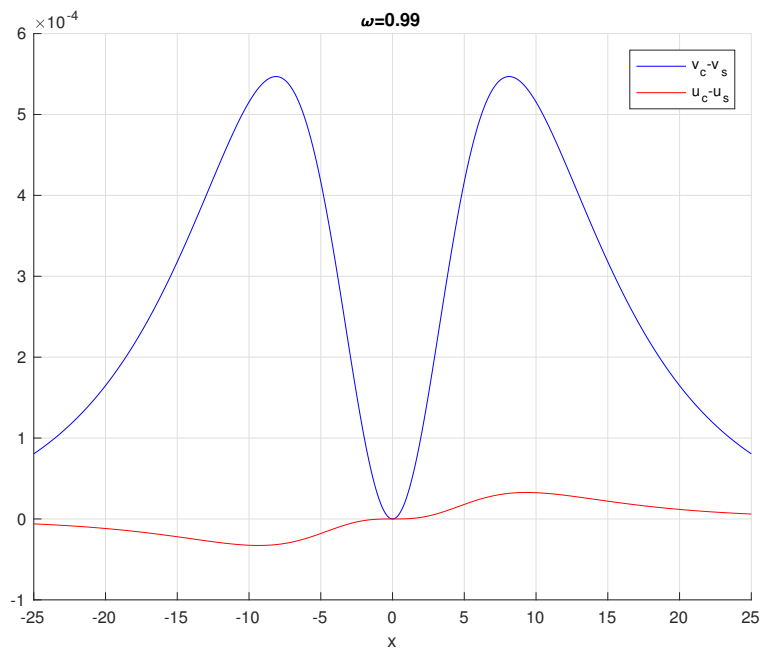
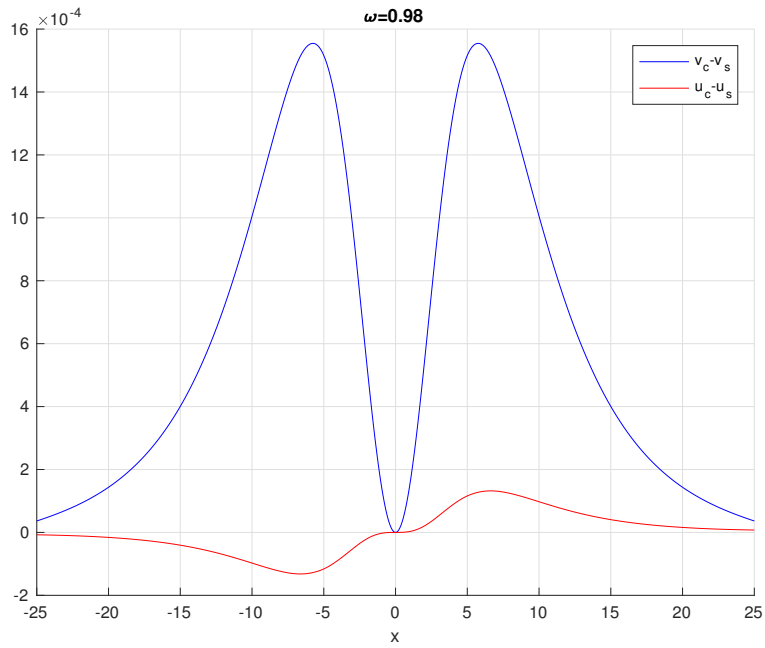


Figure 4.2: Differences of the profile functions between the Soler model and Coulomb model for the frequency ω close to $m = 1$.

Since the even profile functions (v_s and v_c) are much greater than the odd profile functions (u_s

and u_c), the dominant term in the matrix above is $v_s^2 + v_c^2$. We know that $v_s^2, v_c^2 \leq 2(m - \omega)$. Obviously, the difference will go to zero as $\omega \rightarrow m$. If we consider \mathbf{L}_c as a perturbed operator of \mathbf{L}_s , then we expect to find the perturbed eigenvalues (if they survive) in a small neighborhood of $2\omega i$ taking into account the size of the perturbation $V_s - V_c$.

We mimic the process of the 1D Soler model [19] to construct the Evans functions for the toy Coulomb model. Suppose that λ is an eigenvalue of $\mathbf{J}\mathbf{L}_c$ and the corresponding eigenfunction is $R \in \mathbb{R}^4$ such that $\lambda R = \mathbf{J}\mathbf{L}_c R$. The ‘‘even’’ and ‘‘odd’’ subspaces defined in **Section 2.3.3** are also invariant under the action of $\mathbf{J}\mathbf{L}_c$. We use these two subspaces X^\diamond and X^\bullet to decompose $L^2(\mathbb{R}, \mathbb{C}^4)$. By Weyl’s theorem, we know that \mathbf{L}_s and \mathbf{L}_c have the same Jost solutions, namely the solutions to $\lambda J = (-\alpha + m\mathbf{J}\beta - \omega\mathbf{J})J$. They can be written explicitly as

$$J_1 = \begin{bmatrix} -\xi_1 \\ i\lambda - m + \omega \\ \xi_1 \\ \lambda - i(m - \omega) \end{bmatrix} e^{-i\omega\xi_1}, \quad J_2 = \begin{bmatrix} \xi_2 \\ i\lambda - m + \omega \\ -\xi_2 \\ \lambda + i(m - \omega) \end{bmatrix} e^{-i\omega\xi_2},$$

where

$$\xi_1 = \sqrt{(\omega - i\lambda)^2 - m}, \quad \xi_2 = \sqrt{(\omega + i\lambda)^2 - m}, \quad (4.26)$$

with negative imaginary parts. We define the Evans functions by

$$E_{X^\diamond}(\lambda) = \det(R_1, R_3, J_1, J_2), \quad (4.27)$$

$$E_{X^\bullet}(\lambda) = \det(R_2, R_4, J_1, J_2), \quad (4.28)$$

on X^\diamond and X^\bullet , respectively, where $R_j(x)$, $1 \leq j \leq 4$, are the solutions to the equation $\lambda R = \mathbf{J}\mathbf{L}_c R$

with the following initial data at $x = 0$:

$$R_1|_{x=0} = \begin{bmatrix} 1 \\ 0 \\ 0 \\ 0 \end{bmatrix}, \quad R_2|_{x=0} = \begin{bmatrix} 0 \\ 1 \\ 0 \\ 0 \end{bmatrix}, \quad R_3|_{x=0} = \begin{bmatrix} 0 \\ 0 \\ 1 \\ 0 \end{bmatrix}, \quad R_4|_{x=0} = \begin{bmatrix} 0 \\ 0 \\ 0 \\ 1 \end{bmatrix}.$$

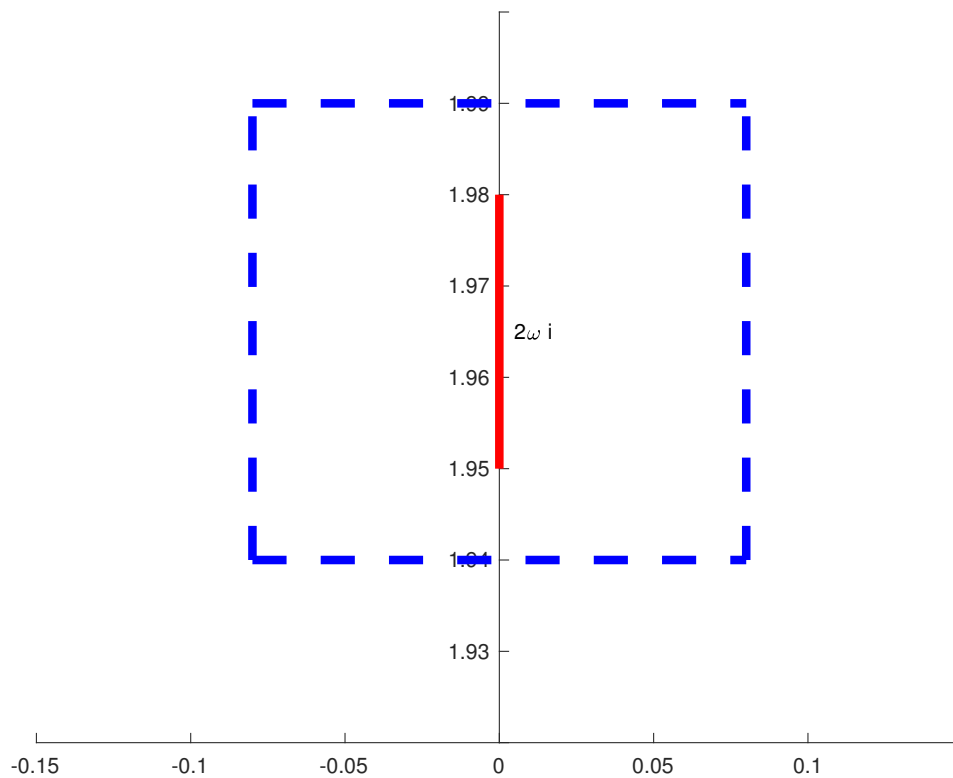


Figure 4.3: The eigenvalues are searched in the region bounded by the blue dash lines for the frequency $\omega \in (0, 975m, 0.99m)$. The red interval represents the values $2\omega i$ corresponding to $\omega \in (0, 975m, 0.99m)$.

By the numerical computation, there are no eigenvalues for $\omega \in (0, 975m, 0.99m)$ in the re-

gion bounded by the blue dash lines in the Figure 4.3. In this case, the roots of the Evans functions no longer correspond to the eigenvalues. We will show that the root of the Evans function corresponding to the eigenvalue $2\omega i$ in the Soler model is now located on the non-physical Riemann sheet corresponding to the Jost solutions with the exponential growth at infinity, so that the toy Coulomb model remains spectrally stable. We define the Evans function on this Riemann sheet by

$$\tilde{E}_{X^\bullet}(\lambda) = \det \left(R_1, R_3, \tilde{J}_1, \tilde{J}_2 \right), \quad (4.29)$$

$$\tilde{E}_{X^\circ}(\lambda) = \det \left(R_2, R_4, \tilde{J}_1, \tilde{J}_2 \right), \quad (4.30)$$

where

$$\tilde{J}_1 = \begin{bmatrix} -\xi_1 \\ i\lambda - m + \omega \\ \xi_1 \\ \lambda - i(m - \omega) \end{bmatrix} e^{i\omega\xi_1}, \quad \tilde{J}_2 = \begin{bmatrix} \xi_2 \\ i\lambda - m + \omega \\ -\xi_2 \\ \lambda + i(m - \omega) \end{bmatrix} e^{i\omega\xi_2},$$

and $\xi_{1,2}$ and R_i , $i = 1, 2, 3, 4$ are same defined as before. Then the roots of \tilde{E} are resonances, which are corresponding to the Jost solutions with the exponential growth at infinity.

According to Figure 4.4, there are two resonances in the first quadrant (containing the upper half imaginary axis) for $\omega \in (0.978m, 0.99m)$. One is in the interval $(i(m + \omega), i\infty)$, in fact just above $(m + \omega)i$, which must be corresponding to the resonance near the threshold $i(m + \omega)$ in the 1D Soler model (see [19]). The other one has nonzero real and imaginary parts, which is not present on the Riemann sheet corresponding to the Jost solutions with the exponential growth at infinity for the 1D Soler model. Thus, the resonance corresponds to the deformation of the eigenvalue $2\omega i$ from the 1D Soler model.

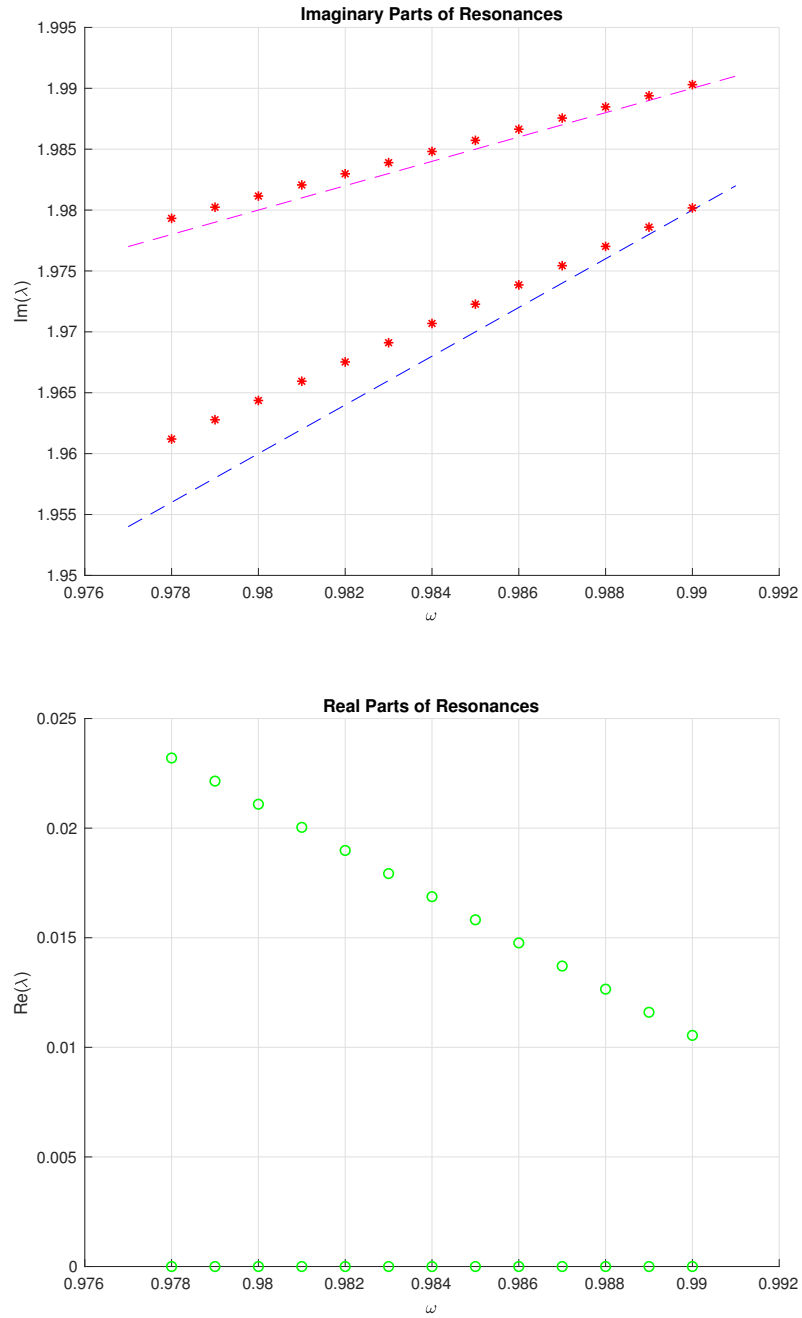


Figure 4.4: Dependence of the imaginary (red asterisks) and real (green circles) parts of resonances in the toy Coulomb model. The pink dash line and blue dash line stand for the threshold $(m + \omega)i$ and the value $2\omega i$, respectively.

4.5 Conclusion

We consider a 1D toy model which is analogous to NLD with Coulomb-type self-interaction. We show that there exist solitary wave solutions for the frequency $\omega \in (0, m)$. Due to the absence of the $SU(1, 1)$ symmetry, the linearized operator JL_c does not have the eigenvalue $2\omega i$. We compare this linearized operator to the one from the 1D Soler model. Since the difference is quite small in the nonrelativistic limit, we anticipate that eigenvalues (if exist) will be close to $2\omega i$. The numerics demonstrate that there are no eigenvalues in the region of $2\omega i$. We know that 1D Soler model is spectrally stable. The nonexistence of eigenvalues near $2\omega i$ in the nonrelativistic limit implies that the spectral stability persists in the toy Coulomb model in spite of the absence of the $SU(1, 1)$ symmetry.

The reason for the absence of an eigenvalue near $2\omega i$ is that the corresponding root of the Evans function no longer corresponds to an eigenvalue. According to the numerics, it is now located on the non-physical Riemann sheet corresponding to the Jost solutions with the exponential growth at infinity; in other words, this root of the Evans function now corresponds to a resonance.

5. SUMMARY

In Chapter 2, we study the 2D Soler model by using the Evans function technique. We show that the solitary wave solutions to the model are spectrally stable when the frequency $\omega \in (0.121m, m)$, and are linearly unstable when the frequency $\omega \in (0, 0.121m)$.

In Chapter 3, we study the 3D Soler model via the similar approach to that for the 2D Soler model. However, only the perturbation with the same angular dependence as that of the solitary waves is considered due to the complexity of the 3D model. We show that the solitary waves are linearly unstable when $\omega \in (0.936m, m)$, and that the positive eigenvalue λ , the one responsible for the linear instability, collides at the origin with $-\lambda$ when $\omega = 0.936m$ and for $\omega < 0.936m$ these eigenvalues move onto the imaginary axis, no longer causing the instability. For $\omega \in (0, 0.936m)$, we expect to obtain a definite result in the future.

In Chapter 4, we consider a toy Coulomb type model. We show that in the nonrelativistic limit it does not have the eigenvalue $2\omega i$ and has no eigenvalue near $2\omega i$, either. Therefore, the spectral stability persists in spite of the absence of the $\text{SU}(1, 1)$ symmetry. The reason for the absence of eigenvalues near $2\omega i$ is that the corresponding root of the Evans function becomes a resonance.

REFERENCES

- [1] J. Cuevas-Maraver, P. G. Kevrekidis, A. Saxena, A. Comech, and R. Lan, “Stability of solitary waves and vortices in a 2D nonlinear Dirac model,” *Phys. Rev. Lett.*, vol. 116, 2016.
- [2] P. Dirac, “The quantum theory of the electron,” *Proc. R. Soc. Lond. Ser. A*, vol. 117, pp. 610–624, 1928.
- [3] A. Pais, *Niels Bohr’s Times*. Oxford: Oxford University Press, 1991.
- [4] B. Fedosov, “Index theorems,” in *Partial Differential Equations, VIII*, vol. 65 of *Encyclopaedia Math. Sci.*, ch. Index Theorems, Springer-Verlag Berlin Heidelberg, 1996.
- [5] D. D. Ivanenko, “Notes to the theory of interaction via particles,” *Sov. Phys. JETP*, vol. 13, 1938.
- [6] A. Rañada, “Classical nonlinear Dirac field models of extended particles,” in *Quantum theory, groups, fields and particles (editor A.O. Barut)*, Amsterdam: Reidel, 1983.
- [7] R. Finkelstein, R. LeLevier, and M. Ruderman, “Nonlinear spinor fields,” *Phys. Rev.*, vol. 83, pp. 326–332, Jul 1951.
- [8] W. Heisenberg, “Quantum theory of fields and elementary particles,” *Rev. Mod. Phys.*, vol. 29, 1957.
- [9] W. E. Thirring, “A soluble relativistic field theory,” *Ann. Phys.*, vol. 3, 1958.
- [10] S. Coleman, “Quantum sine-Gordon equation as the massive Thirring model,” *Phys. Rev. D*, vol. 11, pp. 2088–2097, 1975.
- [11] M. Soler, “Classical, stable, nonlinear spinor field with positive rest energy,” *Phys. Rev. D*, vol. 1, pp. 2766–2769, 1970.
- [12] D. J. Gross and A. Neveu, “Dynamical symmetry breaking in asymptotically free field theories,” *Phys. Rev. D*, vol. 10, pp. 3235–3253, Nov 1974.

- [13] S. Y. Lee and A. Gavrielides, “Quantization of the localized solutions in two-dimensional field theories of massive fermions,” *Phys. Rev. D*, vol. 12, pp. 3880–3886, Dec 1975.
- [14] J. Shatah and W. Strauss, “Instability of nonlinear bound states,” *Comm. Math. Phys.*, vol. 100, no. 2, pp. 173–190, 1985.
- [15] K. Ablowitz and H. Segur, *Solitons and Inverse Scattering Transform*. SIAM, Philadelphia, 1981.
- [16] T. Cazenave and L. Vázquez, “Existence of localized solutions for a classical nonlinear Dirac field,” *Commun. Math. Phys.*, pp. 35–47, 1986.
- [17] F. Merle, “Existence of stationary states for nonlinear Dirac equations,” *J. Differential Equations*, pp. 50–68, 1988.
- [18] M. J. Esteban and E. Séré, “Stationary states of the nonlinear Dirac equation: a variational approach,” *Commun. Math. Phys.*, pp. 323–350, 1995.
- [19] G. Berkolaiko and A. Comech, “On spectral stability of solitary waves of nonlinear dirac equation in 1D,” *Math. Model. Nat. Phenom.*, vol. 7, no. 2, pp. 13–31, 2012.
- [20] D. Edmunds and D. Evans, *Spectral Theory and Differential Operators*. Oxford Mathematical Monographs, Oxford: Oxford University Press, 1987.
- [21] M. Grillakis, J. Shatah, and W. Strauss, “Stability theory of solitary waves in the presence of symmetry. I,” *J. Funct. Anal.*, vol. 74, no. 1, pp. 160–197, 1987.
- [22] A. A. Kolokolov, “Stability of the dominant mode of the nonlinear wave equation in a cubic medium,” *J. Appl. Mech. Tech. Phys.*, vol. 14, pp. 426–428, 1973.
- [23] W. A. Strauss, “Existence of solitary waves in higher dimensions,” *Comm. Math. Phys.*, vol. 55, no. 2, pp. 149–162, 1977.
- [24] H. Berestycki and P.-L. Lions, “Nonlinear scalar field equations. I. Existence of a ground state,” *Arch. Rational Mech. Anal.*, vol. 82, no. 4, pp. 313–345, 1983.

- [25] J. Shatah, “Stable standing waves of nonlinear Klein-Gordon equations,” *Comm. Math. Phys.*, vol. 91, no. 3, pp. 313–327, 1983.
- [26] J. Shatah, “Unstable ground state of nonlinear Klein-Gordon equations,” *Trans. Amer. Math. Soc.*, vol. 290, no. 2, pp. 701–710, 1985.
- [27] M. Grillakis, “Linearized instability for nonlinear Schrödinger and Klein-Gordon equations,” *Comm. Pure Appl. Math.*, vol. 41, pp. 747–774, 1988.
- [28] M. Grillakis, J. Shatah, and W. Strauss, “Stability theory of solitary waves in the presence of symmetry. II,” *J. Funct. Anal.*, vol. 94, no. 2, pp. 308–348, 1990.
- [29] A. Soffer and M. I. Weinstein, “Multichannel nonlinear scattering for nonintegrable equations,” *Comm. Math. Phys.*, vol. 133, no. 1, pp. 119–146, 1990.
- [30] A. Soffer and M. I. Weinstein, “Multichannel nonlinear scattering for nonintegrable equations. II. The case of anisotropic potentials and data,” *J. Differential Equations*, vol. 98, no. 2, pp. 376–390, 1992.
- [31] A. Soffer and M. I. Weinstein, “Resonances, radiation damping and instability in Hamiltonian nonlinear wave equations,” *Invent. Math.*, vol. 136, no. 1, pp. 9–74, 1999.
- [32] S. Cuccagna, “A survey on asymptotic stability of ground states of nonlinear Schrödinger equations,” in *Dispersive nonlinear problems in mathematical physics*, vol. 15 of *Quad. Mat.*, pp. 21–57, Dept. Math., Seconda Univ. Napoli, Caserta, 2004.
- [33] A. Comech, S. Cuccagna, and D. E. Pelinovsky, “Nonlinear instability of a critical traveling wave in the generalized Korteweg-de Vries equation,” *SIAM J. Math. Anal.*, vol. 39, no. 1, pp. 1–33, 2007.
- [34] M. I. Weinstein, “Existence and dynamic stability of solitary wave solutions of equations arising in long wave propagation,” *Comm. PDEs*, vol. 12, pp. 1133–1173, 1987.
- [35] V. Georgiev and M. Ohta, “Nonlinear instability of linearly unstable standing waves for nonlinear Schrödinger equations,” *J. Math. Soc. Japan*, vol. 64, no. 2, pp. 533–548, 2012.

- [36] N. Boussaïd and S. Cuccagna, “On stability of standing waves of Nonlinear Dirac equations,” *Commun. Part. Diff. Eq.*, vol. 37, 2012.
- [37] E. E. Pelinovsky and A. Stefanov, “Asymptotic stability of small gap solitons in nonlinear Dirac equations,” *J. Math. Phys.*, 2012.
- [38] A. Comech, T. V. Phan, and A. Stefanov, “Asymptotic stability of solitary waves in generalized gross–neveu model,” *Annales de l’Institut Henri Poincaré*, pp. 157–196, 2017.
- [39] A. Contretas, E. E. Pelinovsky, and Y. Shimabukuro, “ l^2 orbital stability of Dirac solitons in the massive thirring model,” *Lett. Math. Phys.*, pp. 227–255, 2016.
- [40] E. E. Pelinovsky and Y. Shimabukuro, “Orbital stability of Dirac solitons,” *Lett. Math. Phys.*, pp. 21–41, 2014.
- [41] M. Balabane, T. Cazenave, A. Douady, and F. Merle, “Existence of excited states for a nonlinear Dirac field,” *Commun. Math. Phys.*, vol. 64, pp. 153–176, 1988.
- [42] J. Evans, “Nerve axon equations, i: Linear approximations,” *Indiana U. Math. J.*, vol. 21, pp. 877–955, 1972.
- [43] J. Evans, “Nerve axon equations, ii: Stability at rest,” *Indiana U. Math. J.*, vol. 22, pp. 75–90, 1972.
- [44] J. Evans, “Nerve axon equations, iii: Stability of the nerve impulse,” *Indiana U. Math. J.*, vol. 22, pp. 577–594, 1972.
- [45] J. Evans, “Nerve axon equations, iv: The stable and unstable impulse,” *Indiana U. Math. J.*, vol. 24, pp. 1169–1190, 1975.
- [46] C. Jones, “Stability of the travelling wave solutions of the Fitzhugh–Nagumo system,” *Trans. AMS*, vol. 286, no. 2, pp. 431–469, 1984.
- [47] J. Alexander, R. Gardner, and C. Jones, “A topological invariant arising in the stability analysis of traveling waves,” *J. Reine Angew. Math.*, vol. 410, pp. 167–212, 1990.

- [48] R. Pego and M. Weinstein, “Eigenvalues, and instabilities of solitary waves,” *Philos. Trans. Royal Soc. A*, vol. 340, no. 1656, pp. 47–94, 1990.
- [49] R. Greene and S. Krantz, *Function Theory of One Complex Variable*, vol. 40 of *Graduate Studies in Mathematics*. Providence, Rhode Island: American Mathematical Society, 2006.
- [50] N. Boussaid and A. Comech, “Nonrelativistic asymptotics of solitary waves in the Dirac equation with the Soler-type nonlinearity,” *SIAM J. Math. Anal.*, vol. 49, no. 4, pp. 2527–2572, 2017.
- [51] A. Comech, M. Guan, and S. Gustafson, “On linear instability of solitary waves for the nonlinear Dirac equation,” *Ann. Inst. H. Poincaré Anal. Non Linéaire*, vol. 31, no. 3, pp. 639–654, 2014.
- [52] N. G. Vakhitov and A. A. Kolokolov, “Stationary solutions of the wave equation in the medium with nonlinearity saturation,” *Radiophys. Quantum Electron.*, vol. 16, pp. 783–789, 1973.
- [53] G. Berkolaiko, A. Comech, and A. Sukhtayev, “Vakhitov-Kolokolov and energy vanishing conditions for linear instability of solitary waves in models of classical self-interacting spinor fields,” *Nonlinearity*, vol. 28, no. 3, pp. 577–592, 2015.